



**PARAMETERS FOR CALCULATION TOOL DIMENSIONING A SHEAVE IN  
CRANES ROPE SYSTEM**

Lappeenranta–Lahti University of Technology LUT

Master's programme in Mechanical Engineering, Master's thesis

2022

Matti Koskinen

Examiner: Prof. Timo Björk

M. Sc. (Tech) Esa Ojapalo

## ABSTRACT

Lappeenranta–Lahti University of Technology LUT

LUT School of Energy Systems

Mechanical Engineering

Matti Koskinen

### **Parameters for calculation tool dimensioning a sheave in cranes rope system**

Master's thesis

2022

65 pages, 38 figures, 4 tables and 5 appendices

Examiners: Prof. Timo Björk

M. Sc. (Tech) Esa Ojapalo

**Keywords:** Finite element analysis, FEM, Sheave, crane, rope system, contact pressure, FEMAP

The aim of this research was to study how contact pressure is distributed from a rope to a sheave, as well as to study how the stress is further distributed into the structure, especially the welds. Contact pressure was studied using finite element method in FEMAP/NASTRAN software. Stress distributions in the cross sections were studied using 2D finite element models and cut open 3D models. Fatigue was studied by comparing nominal stress method to effective notch stress method. Previous research suggests that the contact pressure should be constant along the groove. Principal stresses should be highest near hub-web connection.

The most problematic part of the research was connection between the rope and the sheave. As rope is difficult to model realistically, cylindrical model with low elastic modulus was used. Issue with rope is that it has very low bending resistance but high elastic modulus in tensile loading. By using low modulus of elasticity material model, deformations are large, but contact acts as it should. Contact pressure distribution in the curve was mostly constant, but the pressure had discontinuities in the groove. Discontinuities might be caused by stretching of the rope elements or elements in either body not being smooth. If discontinuities were filtered, contact pressure was in the same magnitude as equations from literature suggests. Von Mises stress was similar with finite element analysis as literature references.

Contact pressure and stress distribution result could be used to develop calculation tool according to SFS-EN-13001.

## TIIVISTELMÄ

Lappeenrannan–Lahden teknillinen yliopisto LUT

LUT Energiajärjestelmät

Konetekniikka

Matti Koskinen

**Mitoitusparametrit laskentatyökalulle nosturin köysijärjestelmässä olevalle köysipyörälle**

Konetekniikan Diplomityö

2022

65 sivua, 38 kuvaa, 4 taulukkoa and 5 liitettä

Tarkastajat: Prof. Timo Björk

DI. Esa Ojapalo

Avainsanat: Finite element analysis, FEM, Sheave, crane, rope system, contact pressure, FEMAP

Tämän diplomityön tarkoituksena oli tutkia, kuinka pintapaine jakautuu köydestä köysipyörään, sekä tutkia kuinka jännitys leviää siitä pyörän rakenteeseen, varsinkin hitseihin. Pintapainetta tutkittiin elementtimenetelmällä FEMAP/NASTRAN ohjelmistolla. Jännitys jakaumia poikkileikkauksessa tutkittiin 2D-malleilla elementtimenetelmällä ja auki leikatuilla 3D-malleilla. Väsymistä tutkittiin vertaamalla nimellisen jännityksen menetelmää tehollisen lovi-jännityksen menetelmään. Aiempi tutkimus viittaa, että pintapaine olisi vakio uran pituussuunnassa. Pääjännitysten tulisi olla suurimpia napa-uuma liitoksessa.

Ongelmallisin osa tutkimusta oli kontakti köyden ja uran väillä. Koska köysi on vaikea mallintaa realistisesti, sylinterin muotoista mallia, jolla on matala kimmokerroin, käytettiin laskennassa. Ongelma johtuu köyden suuresta kimmokertoimesta vetosuunnassa, joka on matala taivutussuunnassa. Käyttämällä pientä kimmokerrointa siirtymät ovat suuria, mutta kontakti käyttäytyy realistisesti. Suurimmaksi osaksi pintapaine jakautui tasaisesti, mutta urassa oli epäjatkuvuuskohtia. Epäjatkuvuudet saattavat johtua köyden elementtien venymisestä, tai elementtien liian suuresta käyryydestä. Jos epäjatkuvuudet suodatetaan, pintapaineen arvo on samaa luokkaa kirjallisuuden ehdottamien arvojen kanssa. Von Mises jännitys jakauma vastaa kirjallisten lähteiden viittauksia.

Pintapaineen ja jännitysten jakaumia voitiin käyttää laskentatyökalun kehittämiseen standardin SFS-EN-13001 mukaisesti.

## Table of contents

Abstract

Symbols and abbreviations

1. Introduction .....	12
1.1. Research problem and research questions.....	12
1.2. Objective of work.....	13
2. Design of sheave.....	15
2.1. Design of a sheave according to SFS-EN-13001 .....	15
3. Finite element analysis of sheave .....	25
3.1. Contact pressure distribution along the groove length.....	25
3.2. Stresses in sheave cross section .....	33
3.3. Fatigue analysis using FE-analysis .....	35
4. Results and development of the calculation tool.....	37
4.1. Analysis for the pressure distribution along the groove length.....	37
4.2. Analysis for the pressure distribution along the groove width .....	43
4.3. Horizontal forces .....	47
4.4. Issues in the FE-models of pressure distribution .....	48
4.5. Developing the calculation tool .....	51
4.5.1. Contact pressure.....	51
4.6. Fatigue analysis .....	55
5. Conclusions and evaluation .....	58
5.1. Reliability and validity of the study .....	60
5.2. Further studies .....	60
6. Summary.....	62
References.....	63

Appendices

Appendix 1. FE-models of 135° and 90° winding angle sheaves.

Appendix 2. Von Mises stress distribution in 135° and 90° sheave models.

Appendix 3. Unfiltered contact pressure curve for 135° winding angle.

Appendix 4. Unfiltered contact pressure curve for 90° winding angle.

Appendix 5. Transverse contact pressure curves.

## SYMBOLS AND ABBREVIATIONS

$a$	Vertical acceleration of load (m/s)
$a_w$	Factor for limit weld stress
$D$	Diameter of sheave (mm)
$d$	Diameter of rope (mm)
$E$	Modulus of elasticity (MPa)
$F_h$	Horizontal force (N)
$F_u$	Load capacity of rope (N)
$F_{Sd,s}$	Limit fatigue design rope force (N)
$F_{Rd,s}$	Limit design rope force, static (N)
$f_{S1}$	Rope reeving efficiency
$f_{S2}$	Fall angle factor
$f_{S3}$	Horizontal load factor
$f_{Rd,\sigma}$	Design limit stress (MPa)
$f_f$	Further influences factor
$f_{f6}$	Groove radius factor
$f_{f7}$	Rope type factor
$f_y$	Tensile strength (MPa)
$f_{uw}$	Ultimate tensile strength of base material
$g$	Gravitational acceleration (m/s <sup>2</sup> )
$i$	Stress cycle
$K_t$	Notch factor
$k_m$	Spectrum factor
$k_r$	Spectrum factor
$m$	Slope constant of S-N curve
$N_t$	Number of stress ranges in lifetime
$N_{ref}$	Reference number of stress ranges
$n_i$	Number of stress ranges in cycle $i$
$n_s$	Number of fixed sheaves
$p_0$	Line pressure (N/mm)
$p_1$	Contact pressure (N <sup>2</sup> /mm)

$R_{Dd}$	Reference ratio
$r_g$	Radius of the groove
$s_m$	Stress history parameter
$T_0$	Rope tension (N)
$t$	Rope type factor
$v$	Number of stress ranges in a cycle
$v_r$	Relative number of stress fluctuations
$\gamma$	Angle between gravity and rope (radians)
$\gamma_{RM}$	Material factor
$\gamma_m$	Resistance factor
$\gamma_{mf}$	Resistance factor of a detail
$\gamma_{rb}$	Rope resistance factor
$\gamma_{rf}$	Rope resistance factor
$\gamma_{rf}$	Rope resistance factor
$\gamma_p$	Partial safety factor
$\eta_{tot}$	Total rope reeving ratio
$\eta_S$	Efficiency of single sheave
$\nu_p$	Poisson's ratio
$\Delta\sigma$	Maximum stress range (MPa)
$\Delta\sigma_c$	Fatigue class of a detail (MPa)
$\Delta\sigma_i$	Stress range in cycle $i$ (MPa)
$\sigma_{Sd}$	Design stress range (MPa)
$\sigma_{Rd}$	Limit stress range (MPa)
$\varphi$	Dynamic factor
$\varphi_2$	Dynamic factor for unrestrained grounded loads
$\varphi_5$	Dynamic load factor for acceleration

ENS	Effective notch stress
FE	Finite element
FEM	Finite element method



## Figures

Figure 1: Illustration of crane sheave. (Gosan)

Figure 2: Fall angle for a rope system. (SFS-EN-13001-3-2, p.13)

Figure 3: Resistance factor  $\gamma_{mf}$  for sheave welds. (SFS-EN-13001-3-1, p.139)

Figure 4: Fatigue class of the welds. (SFS-EN-13001-3-1, p.173)

Figure 5: Fatigue class of web. (SFS-EN-13001-3-1 p.165)

Figure 6: Definition of factor  $a_w$ . (SFS-EN-13001-3-1, p.135)

Figure 7: Full model of the sheave.

Figure 8: Cross section of the sheave used in FE-calculation.

Figure 9: Contact surfaces in transparent 3D-model of the system.

Figure 10: Connection property for contact elements.

Figure 11: Normal line pressure versus winding angle. (Usabiaga et. al, 2008, p.40)

Figure 12: Illustration of sheave showing line pressure and winding angle. (Usabiaga, et al., 2008, p.36)

Figure 13: FE-model for the welded sheave cross section.

Figure 14: FE-model for the cast sheave cross section.

Figure 15: Web-hub weld and its air gap, hole and rounding's.

Figure 16: Web-groove weld and rounding's at the weld roots.

Figure 17: Von Mises stress in the sheave for 180° winding angle.

Figure 18: Contact pressure distribution in the groove bottom for 180° winding angle.

Figure 19: Contact pressure distribution in the groove bottom for 135° winding angle.

Figure 20: Contact pressure distribution in the groove bottom for 90° winding angle.

Figure 21: Contact pressure in half groove for 180° winding angle element number 1 being rope off point and element number 162 in the middle.

Figure 22: Filtered contact pressure curve in half groove for 180° winding angle element 1 being at the rope off point and element number 133 in the middle.

Figure 23: Contact pressure distribution for 135° winding angle.

Figure 24: Filtered contact pressure distribution for 90° winding angle.

Figure 25: Von Mises stress distribution in welded sheave cross section.

Figure 26: Cut cross section of sheave of full model FE-analysis.

Figure 27: Von Mises stress distribution in cast sheave cross section.

Figure 28: Element numbers in groove cross section.

Figure 29: Contact pressure curve across the groove taken from full FE-model for 180° winding angle.

Figure 30: Deformation of horizontally loaded sheave.

Figure 31: Contact pressure of the horizontally loaded sheave.

Figure 32: Contact pressure distribution in the rope.

Figure 33: Contact pressure in the sheave with contacts master-slave surfaces switched.

Figure 34. Groove dimensions. (SFS-EN-13001-3-2, p.25)

Figure 35. *t*-factor for different types of ropes, (SFS-EN-13001-3-2, p.26)

Figure 36. *t*-factor for different types of ropes, (SFS-EN-13001-3-2, p.26)

Figure 37: Notch stress at the weld root.

Figure 38: Simplified cross section for ENS-analysis.

**Tables**

Table 1: Average contact pressures

Table 2: Suggested maximum contact pressures for manganese steel sheave for regular lay type of ropes. (American iron and steel institute, 1979, p.38)

Table 3: Suggested maximum contact pressures for manganese steel sheave for lang lay type of ropes. (American iron and steel institute, 1979, p.38)

Table 4: Suggested maximum contact pressures for cast iron and carbon steel cast sheave for lang lay type of ropes. (American iron and steel institute, 1979, p.38)

# 1. Introduction

This thesis is done for Konecranes Finland Oy. Konecranes is a provides lifting equipment for use in manufacturing, process industry, shipyards, ports and terminals. The work includes study of stress distribution for constructing a calculation tool for dimensioning a rope sheave according to relevant standards and FE-calculation (finite element) study of sheave. Tools used are FEMAP/NASTRAN for FE-calculation and Siemens NX for 3D-modelling, while the calculation tool is made for Microsoft Excel. Goal of studying contact pressure and stress distributions in sheave is to study its service life, potential optimisation of material usage and further the results can be compared to analyse potential failure compared to other likely failure modes, such as wear or corrosion.

Previous research includes studies about stress distribution in a traction sheave made by Usabiaga, et al. (2008) and Xi, et al. (2016). Research made by Rokita, T. (2016, p.415-424) studies stress distribution in sheave structures. Standards used to design sheaves are SFS-EN-13001-3-1 and SFS-EN-13001-3-2. Previously used standard is FEM 1.001 3<sup>rd</sup> edition. Booklets 3 and 4.

## 1.1. Research problem and research questions

The main research problem of the study is to find stress distributions for creation of a calculation tool for rope sheave used in cranes. To create a reliable calculation tool, contact pressure distribution between rope and sheave needs to be studied, stresses in welds, as well as stress distribution in the cross section of the sheave. Effects of manufacturing and material have a great influence on focus of the research. This thesis focuses on welded steel sheave. Other possible construction materials are cast iron and fibre reinforced polymers. For cast iron sheaves fatigue of welds is not an issue, while for fibre reinforced polymer sheaves wear of the sheave groove is the most consequential factor. From these research problems following research questions are formed:

- What is the contact pressure distribution along the groove, and how can it be reasonably considered in calculation?

- How are the stresses distributed along the cross section of a sheave, and what effect do they have on static and fatigue strength?
- What are stresses in the welds and what are welds fatigue life?
- What are effects of other failure mechanism, such as wear and corrosion?

## 1.2. Objective of work

Objective of this thesis is to create an Excel calculation tool for dimensioning a rope sheave. User should be able to receive dimensions and relevant information about stresses according to input values. Calculation tool is done according to the standard SFS-EN-13001. Stress distribution in the sheave cross section and along the groove is studied using FE-analysis. Observations from stress distribution analysis is considered in the calculation tool. Calculation tool should be able to calculate dimensions and relevant stresses for both static and fatigue loading cases based on input values. Input values for loading include maximum static loading, fatigue loading and winding angle. Secondary objective is to compare nominal stress method used in SFS-EN-13001-3-1 to more complex effective notch stress method for calculating fatigue life of a sheave. Figure 1 shows an example of a sheave.



Figure 1. Illustration of crane sheave. (Gosan)

## 2. Design of sheave

Standard defining requirements for rope systems SFS-EN 13001-3-1 is used as a basis for designing a sheave. SFS-EN 13001-3-1 is a standard for designing steel structures for cranes. Sheaves do not have their own standard unlike SFS-EN 13001-3-2 which is a standard for rope systems in cranes. Even though SFS-EN 13001-3-2 is for rope systems, some of its design methods can be used for design of sheave or calculating rope forces acting on a sheave. SFS-EN-13001-3-3 is a standards for design of wheel/rail contact.

In addition to standards, there has been made some research relevant on sheaves and stress distributions in them. This research includes research made by Usabiaga, et al. (2008) and Xi, et al. (2016). These both research papers focus on traction sheaves that can act force on rope, while pulley type sheaves only guides and changes direction of a rope. More relevant research on sheaves was not available.

### 2.1. Design of a sheave according to SFS-EN-13001

Design standard for sheave design is SFS-EN-13001-3-1. This standard defines design for steel structures for cranes. The other standard that can be used to design sheave is FEM 1.001 3<sup>rd</sup> edition Booklet 3 and Booklet 4. Booklet 3 is meant for calculating stresses, while Booklet 4 is meant for fatigue design. Standard meant for rope systems can be used as well as guidance. Standard for rope systems is SFS-EN-13001-3-2. According to SFS-EN-13001-3-1 (2019, p.19) limit for static strength is defined in following way. Design rope force should create stress smaller than design limit stress.

$$f_{Rd,\sigma} = \frac{f_y}{\gamma_{RM}} \quad (1)$$

where is  $f_y$  yield strength of the material [MPa], according to SFS-EN-13001-3-1 and  $\gamma_{Rm}$  is material factor which is  $\gamma_{Rm} = 0,95$ .

Design rope force is calculated from mass of the load considering mechanical advantage, dynamic factor and safety factor. It is calculated using following equation, according to EN-13001-3-2 (2014, p.10).

$$F_{Sd,s} = \frac{m_{Hr}g}{n_m} \varphi f_{S1} f_{S2} f_{S3} \gamma_p \gamma_n \quad (2)$$

where  $m_{Hr}$  is mass of the load [kg],  $g$  is gravitational acceleration [ $\frac{m}{s^2}$ ],  $n_m$  is mechanical advantage,  $f_{S1}: f_{S3}$  are rope force increasing factors,  $\gamma_p$  is partial safety factor and  $\gamma_n$  is the risk factor defined in SFS-EN-13001-2.

Dynamic factor  $\varphi$  is a factor that considers increases in the rope force due to acceleration or deceleration of the load. For calculation,  $\varphi$  can be unrestrained grounded load or accelerated or decelerated load. For hoisting of unrestrained grounded load,  $\varphi$  is defined according to following equation in SFS-EN-13001-3-2 (2014, p.11-12).

$$\varphi = \varphi_2 \quad (3)$$

where  $\varphi_2$  is dynamic factor for unrestrained grounded loads defined in SFS-EN-13001-2.

For accelerating or decelerating load  $\varphi$  is defined according to following equation in SFS-EN-13001-3-2 (2014, p.12).

$$\varphi = 1 + \varphi_5 \frac{a}{g} \quad (4)$$

where  $\varphi_5$  is dynamic load factor for acceleration defined in SFS-EN-13001-2 and  $a$  is vertical acceleration of the load [ $\frac{m}{s^2}$ ].



Factor  $f_{S1}$  stands for rope reeving efficiency. It is defined in SFS-EN-13001-3-2 (2014, p.12). as shown in following way:

$$f_{S1} = \frac{1}{\eta_{tot}} \quad (5)$$

where  $\eta_{tot}$  is total rope reeving ratio, which is calculated according to following equation. (SFS-EN-13001-3-2, 2014, p.12)

$$\eta_{tot} = \frac{(\eta_S)^{n_s}}{n_m} \frac{1 - (\eta_S)^{n_m}}{1 - \eta_S} \quad (6)$$

where  $\eta_S$  is efficiency of single sheave and  $n_s$  is the number of fixed sheaves.

$f_{S2}$  is a factor that considers fall angle of the rope. Fall angle for each sheave can differ meaning  $f_{S2}$  factor will be different. Largest angle found in the system should be used for calculation.  $f_{S2}$  is defined according to SFS-EN-13001-3-2 (2014, p.13). shown in the following equation.

$$f_{S2} = \frac{1}{\cos \beta_{max}} \quad (7)$$

where  $\beta_{max}$  is the maximum fall angle [radians]. Illustration of the system is shown in figure 2.

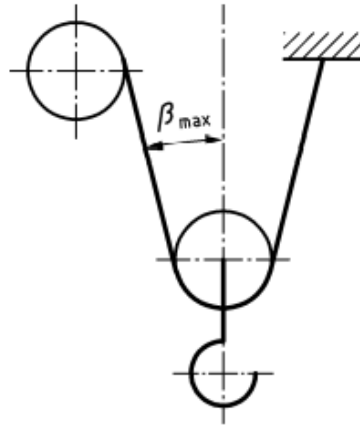


Figure 2. Fall angle for a rope system. (SFS-EN-13001-3-2, 2014, p.13)

$f_{S3}$  is a factor used to factor in horizontal loads to the rope system. Horizontal loads are caused by crane or trolley acceleration or wind.  $f_{S3}$  is calculated according to SFS-EN-13001-3-2 (2014, p.14) as shown in the equation following.

$$f_{S3} = 1 + \frac{F_h}{m_H g \tan \gamma} \leq 2 \quad (8)$$

where  $F_h$  is horizontal force [N] and  $\gamma$  is angle between gravity and the rope [radians].

For fatigue loads similar condition must be met as for static loads shown in equation 1. Equation following shows requirement for fatigue stresses. (SFS-EN-13001-3-1, 2018, p.42)

$$\sigma_{Sd,f} \leq \sigma_{Rd,f} \quad (9)$$

where  $\sigma_{Sd,f}$  is fatigue design stress [MPa] and  $\sigma_{Rd,f}$  is limit fatigue design stress [MPa] according to SFS-EN-13001-3-1 (2018, p.42).

Limit fatigue design stress is calculated according to following equation, defined in SFS-EN-13001-3-1 (2018, p.43).

$$\sigma_{Rd,f} = \frac{\Delta\sigma_c}{\gamma_{mf} \sqrt[m]{s_m}} \quad (10)$$

where  $\Delta\sigma_c$  is fatigue class of the detail,  $\gamma_{mf}$  is resistance factor of the detail for fatigue loads.  $m$  is slope constant of the S-N curve.  $s_m$  is stress history parameter.  $s_m$  is defined by SFS-EN-13001-3-1 (2018, p.43)

History parameter  $s_m$  considers variation in loads and it is defined in the SFS-EN-13001-1. Equation below shows how it defined. (SFS-EN-13001-3-2, 2014, p.21)

$$s_r = k_m v \quad (11)$$

where  $k_m$  is spectrum factor and  $v_r$  is relative number of stress fluctuations.

Welds in the sheave structure are not defined in SFS-EN-13001-3-2, standard SFS-EN-13001-3-1 which defines limit states for steel structures can be used to design welds of the sheave. Proof of the welds can be proven with similar equation to the sheave structure as shown in equation following. (SFS-EN-13001-3-1, 2019, p.42)

$$\sigma_{Sd} \leq \sigma_{Rd} \quad (12)$$

where  $\sigma_{Sd}$  is design stress range for the detail and  $\sigma_{Rd}$  is limit stress range for the detail. Limit stress range  $\sigma_{Rd}$  can be calculated using equation following. (SFS-EN-13001-3-1, 2019, p.42)

$$\sigma_{Rd} = \frac{\Delta\sigma_c}{\gamma_{mf} \sqrt[m]{s_m}} \quad (13)$$

where  $\Delta\sigma_c$  is fatigue class of the detail,  $\gamma_{mf}$  is resistance factor of the detail,  $m$  is slope constant of the S-N-curve for the detail and  $s_m$  is stress history parameter. Definition of  $\gamma_{mf}$  is shown in figure 3. Sheaves are non-fail-safe components that can cause hazards for persons. Both hub and groove welds are not accessible from inside, thus resistance factor for all the welds is  $\gamma_{mf} = 1,25$ . Slope constant  $m$  is typically defined in SFS-EN-13001-3-1 Annex D and Annex H.

Accessibility for inspection	Fail-safe components	Non fail-safe components	
		without hazards for persons	with hazards for persons
Detail accessible without disassembly	1,0	1,05	1,15
Detail accessible by disassembly	1,05	1,10	1,20
Non-accessible detail	N/A <sup>a)</sup>	1,15	1,25
Fail-safe structural details are those, where fatigue cracks do not lead to global failure of the crane or dropping of the load. Cranes working in protected areas with no access to persons are considered to be without hazards to persons. Disassembly means that components must be taken apart or dismantled. A detail is considered to be accessible without disassembly also in cases, where a crack is initiated inside of a closed structure but accessible for detection from outside.			
a) Non-accessible details shall not be considered to be fail-safe.			
b) If a risk coefficient $\gamma_n \geq 1,2$ is applied, this column may be applied to any non fail-safe detail.			

Figure 3. Resistance factor  $\gamma_{mf}$  for sheave welds. (SFS-EN-13001-3-1, 2019, p.139)

Fatigue class  $\Delta\sigma_c$  of the detail is defined in SFS-EN-13001-3-1 Annex D and Annex H. Figure 4 shows the fatigue class 3.8 in SFS-EN-13001-3-1 Annex D for both welds in a sheave. Detail 3.8 corresponds to sheaves welds since they are continuous fully penetrated T-welds, and the loading is mostly similar type as shown in the figure 4. For this detail the slope constant is  $m = 3$ . Fatigue class can be  $\Delta\sigma_c = 112\text{MPa}$ ,  $\Delta\sigma_c = 100\text{MPa}$ ,  $\Delta\sigma_c = 80\text{MPa}$  or  $\Delta\sigma_c = 71\text{MPa}$ . Angle between web and hub causes small bending stress in the web-hub weld. This case is detail number 3.10. Detail number 3.10 has fatigue class of either  $\Delta\sigma_c = 45\text{MPa}$ ,  $\Delta\sigma_c = 71\text{MPa}$ , or  $\Delta\sigma_c = 80\text{MPa}$ . Difference between these is caused by the

weld quality. By having no initial points class can be increased by one class and if shrinkage is restrained the class is downgraded by one. (SFS-EN-13001-3-1, 2019, p.173)

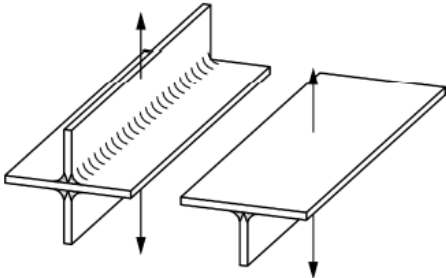
3.8	$m = 3$	<p><b> A1&gt;</b></p>  <p><b>&lt;A1 </b></p> <p>Cross or T-Joint, groove weld, normal stress across the weld</p>	<p>Basic conditions:</p> <ul style="list-style-type: none"> <li>— continuous weld</li> <li>— full penetration weld</li> </ul> <p>Special conditions:</p> <ul style="list-style-type: none"> <li>— automatic welding, no initial points +1 NC</li> <li>— welding with restraint of shrinkage -1 NC</li> </ul>
<b>112</b>		K-weld, quality level B*	
<b>100</b>		K-weld, quality level B	
<b>80</b>		K-weld, quality level C	
<b>71</b>		V-weld with backing, quality level C	

Figure 4. Fatigue class of the welds. (SFS-EN-13001-3-1, 2019, p.173)

Figure 5 shows detail of sheave web and corresponding fatigue class. Fatigue class of the detail is dependent on strength of the material.

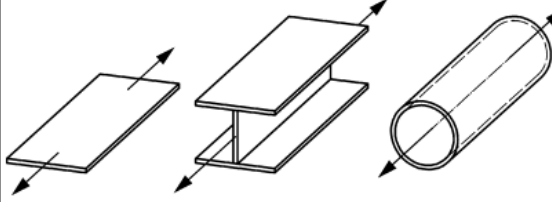
Detail No.	$\Delta\sigma_c$ $\Delta\tau_c$ $N/mm^2$	Constructional detail	Requirements
1.1	$m = 5$	 <p>Plates, flat bars, rolled profiles under normal stresses</p>	General requirements: <ul style="list-style-type: none"> <li>— Rolled surfaces</li> <li>— No geometrical notch effects (e.g. cut outs)</li> <li>— Surface roughness values before surface treatment such as shot blasting</li> </ul>
<b>140</b>	Independent of $f_y$		— Surface condition in accordance with EN 10163 (all parts) classes A1 or C1 (repair welding allowed)
<b>140</b>	$180 \leq f_y \leq 220$		— Surface condition in accordance with EN 10163 (all parts) classes A3 or C3 — Surface roughness $R_z \leq 100 \mu m$ — Edges rolled or machined or no free edges — Any burrs and flashes removed from rolled edges — Surface roughness $R_z \leq 60 \mu m + 1 NC$
<b>160</b>	$220 < f_y \leq 320$		
<b>180</b>	$320 < f_y \leq 500$		
<b>200</b>	$500 < f_y$		
<b>180</b>	$180 \leq f_y \leq 220$		— Surface condition in accordance with EN 10163 (all parts) classes A3 or D3 — Surface roughness $R_z \leq 20 \mu m$
<b>200</b>	$220 < f_y \leq 320$		
<b>225</b>	$320 < f_y \leq 500$		
<b>250</b>	$500 < f_y \leq 650$		
<b>280</b>	$650 < f_y \leq 900$		
<b>315</b>	$900 < f_y$		— Edges machined or no free edges

Figure 5. Fatigue class of web. (SFS-EN-13001-3-1, 2019, p.165)

Stress history parameter  $s_m$  is defined by following equation in SFS-EN-13001-3-1 (2019, p.40).

$$s_m = vk_m \quad (14)$$

where  $v$  number of stress ranges in a cycle defined in equation below and  $k_m$  spectrum factor defined in the next equation. (SFS-EN-13001-3-1, 2019, p.40)

$$v = \frac{N_t}{N_{ref}} \quad (15)$$

where  $N_t$  is number of stress ranges in lifetime of the part and  $N_{ref}$  is reference number of cycles which is  $N_{ref} = 2 \cdot 10^6$ . Number of stress cycles is defined from expected work cycles of the crane. Work cycle has an average rope travel distance. Number of stress cycles in a sheave can be calculated by dividing lifetime rope travel by circumference of the sheave and rope reeving ratio. Diameter of the sheave needs to be known at this point.

$$k_m = \sum_i \left[ \frac{\Delta\sigma_i}{\Delta\sigma} \right]^3 \cdot \frac{n_i}{N_t} \quad (16)$$

where  $n_i$  is number of stress ranges in cycle  $i$ ,  $\Delta\sigma$  is maximum stress range and  $\Delta\sigma_i$  is stress range in cycle  $i$ .

Static strength of the welds is defined by SFS-EN-13001-3-1 (2019, p.135). Limit strength for static stress is defined by equation below.

$$f_{w,Rd} = \frac{a_w f_{uw}}{\gamma_m} \quad (17)$$

where  $a_w$  is a factor depending on material and type of stress,  $f_{uw}$  is ultimate tensile strength of the base material and  $\gamma_m$  is resistance factor. Factor  $a_w$  is defined in figure 6. Factors depending on  $a_w$  are filler material, base material, stress type and type of weld. (SFS-EN-13001-3-1, 2019, p.135)

Type of weld material	Direction of stress	Type of weld	Type of stress	Equation number	$\alpha_w$		
					$f_y \leq 420$ N/mm <sup>2</sup>	$f_y > 420$ $f_y < 930$ N/mm <sup>2</sup>	$f_y \geq 930$ N/mm <sup>2</sup> . <sup>b)</sup>
<b>Matching</b> ( $f_y$ refers to the welded members)	Stress normal to the weld direction	Full penetration weld	Tension or compression	21	1,0		
		Partial penetration weld <sup>a)</sup>	Tension or compression	21	0,90		. <sup>b)</sup>
	Stress parallel to the weld direction	All welds	Shear	21	0,60		. <sup>b)</sup>
<b>Under-matching</b> ( $f_y$ refers to the weld material)	Stress normal to the weld direction	Full penetration weld	Tension or compression	22	0,80	0,85	0,90
		Partial penetration weld <sup>a)</sup>	Tension or compression	22	0,70	0,75	0,80
	Stress parallel to the weld direction	All welds	Shear	22	0,45	0,50	0,50

Figure 6. Definition of factor  $\alpha_w$ . (SFS-EN-13001-3-1, 2019, p.135)

General resistance factor  $\gamma_m$  has value of  $\gamma_m = 1,1$  according to SFS-EN-13001-3-1 (2019, p.122). Nominal strength values for steel grades are defined by table 2 in SFS-EN-13001-3-1 (2019, p.116-117). For sheaves the most important factors when choosing a material are strength properties, formability and hardness. Lower hardness steels can be flame hardened at the groove to reach needed wear resistance. For higher strength steels formability can be an issue.



### 3. Finite element analysis of sheave

To be able to use standards meant to be used, more accurate data about loading on sheave is needed. Previously made research suggests that contact pressure at the groove is close to constant. By understanding maximum and average stresses, and how they are distributed, it should be possible to optimize the structure and minimize failures. Since finite element analysis is approximation, that can have errors, the results should be compared to real life experimental data, or at least theoretical results. Results of finite element experiment should give a numerical factor for winding angle of the rope, confirm stress distributions in web, welds and groove, and give comparison for nominal stress method of welds.

#### 3.1. Contact pressure distribution along the groove length

The main research method in this thesis is finite element method analysis of the structure. Contact pressure distribution is studied to create mathematical relationship between the maximum contact pressure and average contact pressure for different contact angles. The goal is to find a factor for each longitudinal and transverse distribution for each winding angle. Pressure distribution along the curve is used in the calculation tool for sheave dimensioning. Strands and wires of a rope will cause local stresses to be higher than stresses analysed by simplifying the rope. These local stresses are beyond the focus of this research and do not affect dimensioning of a sheave. On the other hand, they can influence wear and should be focus of future research.

FE-model used for the model is full model of a sheave. Full model of the sheave was chosen due to having reasonable analysis time between 10-15 minutes for all analysis cases. Since contact property is non-linear and the analysis type is linear static, the analysis time is mostly dependent on the contact property. A model for sheave is based on simplified model for real sheave with simplifications around the sheave-shaft connection area. Groove and web of the model are identical to the real sheave used basis. Model for rope is a round cylinder shape formed to the shape of the groove. Rope is extended 300mm from connection point between

the rope and the sheave. Elastic modulus used for the rope is 500MPa. Wire ropes have tensile elastic modulus between 40GPa and 140GPa.(Certex, 2022) Very low value for elastic modulus is needed for the rope to carry with correct stress type. With very low values for elastic modulus all the load is carried with membrane stresses, while with higher elastic modulus bending stress is increased. Ropes are meant to have mostly membrane loading. In practice, if rope is modelled with too high elastic modulus, bending stress dominates membrane stress, which leads to all the contact pressure being concentrated on the top of the sheave. Modelling the rope with a very small gap to the groove did not influence the stress distribution for rope with realistic elastic modulus. Gap between the rope and sheave is defined by initial penetration property of the contact, which was zero, thus gap in the model has no effect if the same nodes make contact. Figure 7 shows full model with 4mm meshing, loading and constraints. Figure 8 shows cut cross section of the same model. Appendix 1 shows finite element models for 135° and 90° winding angle. The models are otherwise the same, except winding angle of the rope.

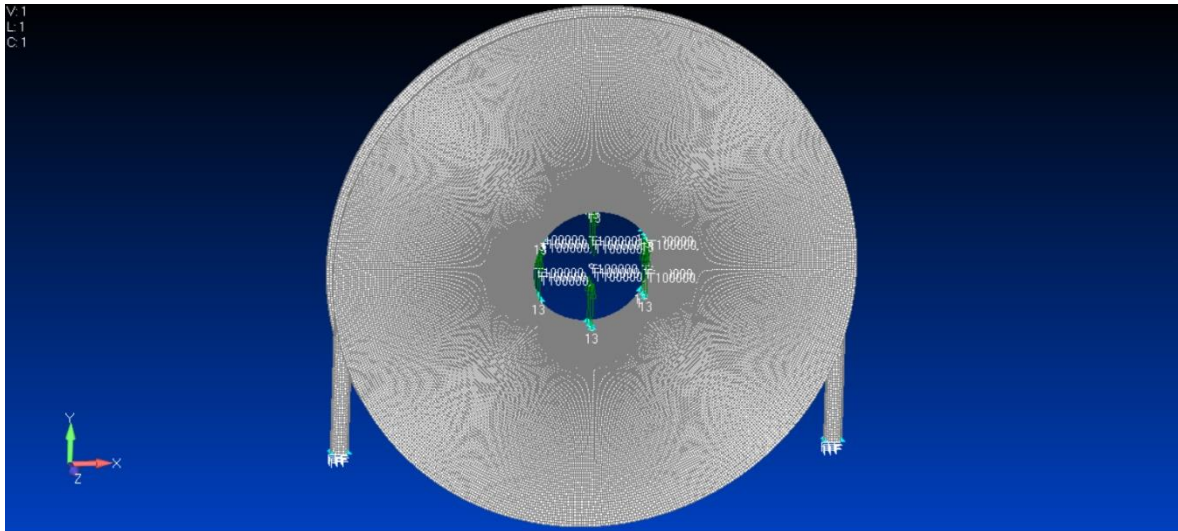


Figure 7. Full model of the sheave. (FEMAP v11.4.2)

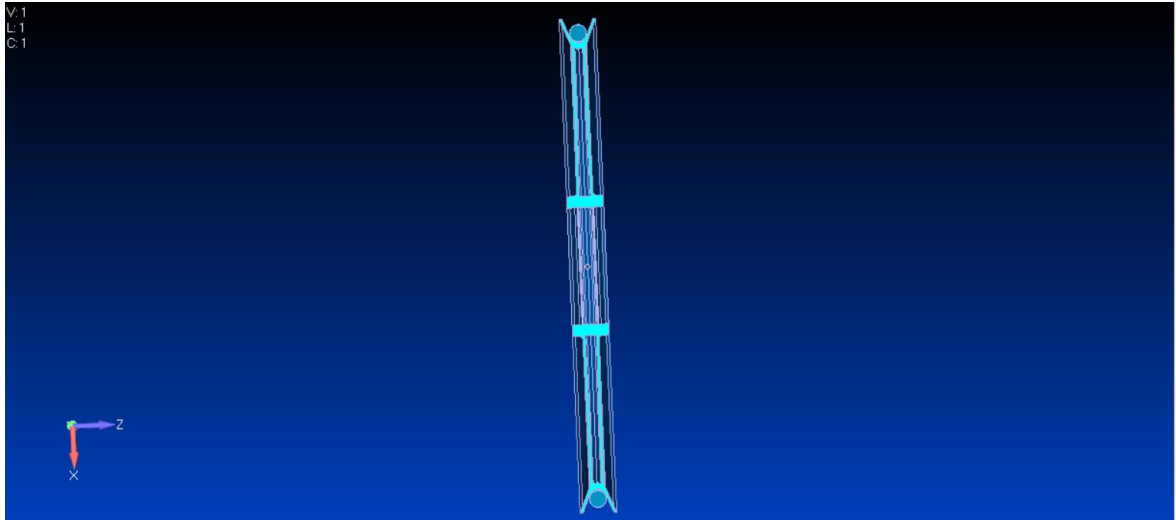


Figure 8. Cross section of the sheave used in FE-calculation. (FEMAP v11.4.2)

Material model for the sheave is linear model of steel. It has elastic modulus of  $E = 210\text{GPa}$  and Poisson's ratio of  $\nu_p = 0,3$ . Elements for both rope and sheave are 8-node solid elements. Element size for both rope and sheave are 4mm. Different element sizes between bodies can interfere with proper transition of stress. Stresses are transferred from rope to the sheave via contact elements. Two surfaces used to connect by contact elements are entire rope surface and groove bottom. Figure 9 shows contact surfaces between rope and sheave. Default properties except maximum contact search distance, that are shown in figure 10, are used for the contact element. Limiting the search distance was needed to make the analysis run through. Without limiting the search distance all the nodes would search contact pair from all the opposing body nodes within the large search distance possibly on every iteration. Large number of nodes searching contact pair from large distance leads to great number of calculations, which led to error of the software.

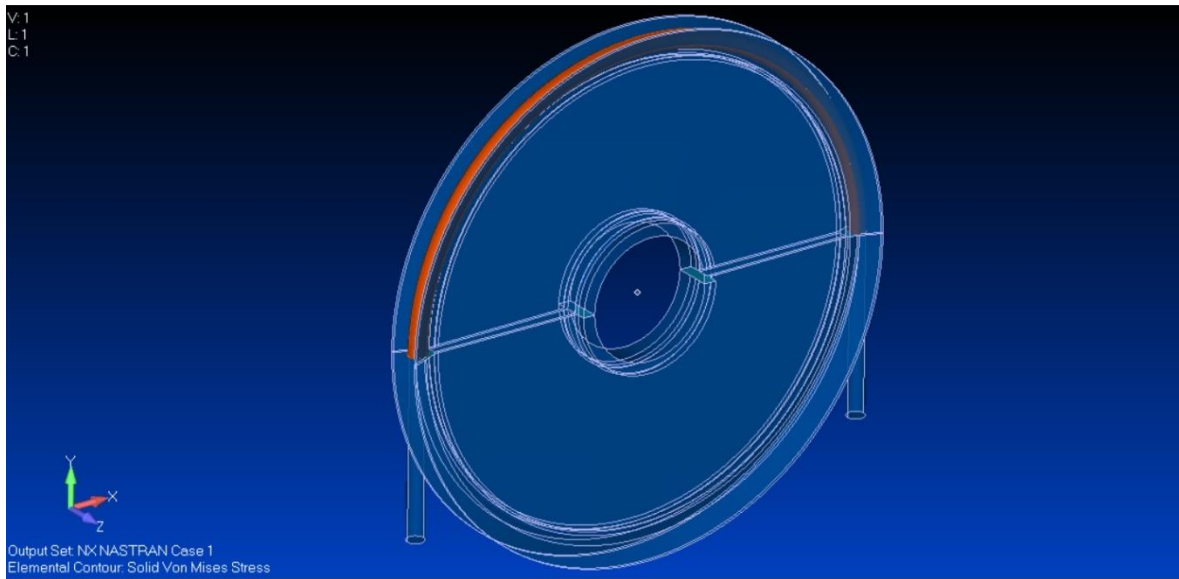


Figure 9. Contact surfaces in transparent 3D-model of the system. (FEMAP v11.4.2)

Define Connection Property

ID: 1 Title: [ ] Connect Type: 0..Contact

Color: 110 Palette... Layer: 3

NX Linear NX Adv Nonlin NX Explicit ABAQUS ANSYS MSC Nastran LS-DYNA NEI Nastr

Contact Pair (BCTSET)

Friction: 0, Min Contact Search Dist: 0, Max Contact Search Dist: 10,

Contact Property (BCTPARM)

Max Force Iterations: 10 Initial Penetration: 0..Calculated

Max Status Iterations: 20 Shell Offset: 0..Include shell thickness

Force Convergence Tol: 0,01 Contact Status: 0..Start from Prev Subcas

Convergence Criteria: 1..Percentage of A Contact Inactive: 0..Can Be Inactive

Num Change For Convergence: 0,02 Shell Z-Offset: 0..Include Z-Offset

Common Contact (BCTPARM) and Glue (BGPARM) Parameters

Glue Type: 2..Weld Penalty Factor Units: 1..1/Length

Eval Order: 2..Medium  Auto Penalty Factor

Refine Source: 2..Refinement Occurs Penalty Autoscale: 1,

Constrain In-Plane Surface Strains Normal Factor: 10,

Generate Contact Preview File Tangential Factor: 1,

Glue Factor: 0,

Glued Contact Property (BGSET)

Search Distance: 0,

Defaults Load... Save... Copy... OK Cancel

Figure 10. Connection property for contact elements.

Master surface in the contact is the sheave and the rope is slave. In FE-analysis master body can penetrate slave body while slave body cannot penetrate master body. In general master body should be flat rather than curved and slave body should have finer mesh. Master body should be stiffer than slave body. As both bodies are curved and have same size mesh, sheave should be master as it is more less flexible as rope. If both surfaces are both masters and

slaves at the same time, neither of the surfaces can penetrate each other. Both surfaces not being able to penetrate each other might improve the contact. (Nam-Ho, 2015, p.414-419)

For a sheave with equal tension in both ends of the rope, line pressure is constant along the groove and calculated by following equation (Usabiaga, et al., 2008). Contact pressure along the groove is  $p_0$  divided by the contact area.

$$p_0 = \frac{2T_0}{D} \quad (18)$$

where  $T_0$  tension of the rope and  $D$  groove bottom diameter of the sheave. Contact pressure of the groove is calculated by equation below.

$$p_1 = \frac{p_0}{d} \quad (19)$$

where  $d$  is diameter of the rope.

Contact pressure can also be calculated using equation below according to Budynas & Nisbett (2011, p.919). These equations assume pressure to be distributed equally in longitudinal and transverse direction which might be too great simplification. Figure 28 shows contact pressure is not constant. These equations do not consider local pressure peaks caused by individual wires either.

$$p_1 = \frac{2T_0}{dD} \quad (20)$$

FE-analysis includes studies of stress distribution with different angles. Analysis is done for three angles: 180°, 135° and 90°. Analysis includes both regular loading case and skew

loading for  $180^\circ$  winding angle. Stress distribution is obtained by plotting nodal contact pressure from bottom of the groove.

Loading for the analysis is 100kN vertical loading on bearing surface of the hub. For skew load case, two nodal loads on groove bottom on opposite sides with magnitude of 2% of rope force are added. Opposite end of the rope is constrained by fixed constraint in the end surface. Loaded surface of the rope is also constrained by limiting translations in X-axis and Y-axis. Rotation of the sheave does not have an influence since contact element between rope and sheave has zero friction.

Previous research on the topic includes research made by Usabiaga, et al. (2008) and Xi, et al. (2016). These both papers study contact pressure along groove of friction sheave, while this study considers pulley type sheaves. While pulley type sheave only changes direction changes direction of the rope force, force is added into the rope system by friction sheave. In friction sheave, friction force is large in the groove, while in pulley sheaves friction force is low. Figure 11 shows pressure distribution along the winding angle according to Usabiaga, et al. (2008, p.40). Figure 12 shows illustration of the sheave used in the same study. It shows winding angle, rope off angles and line pressure.

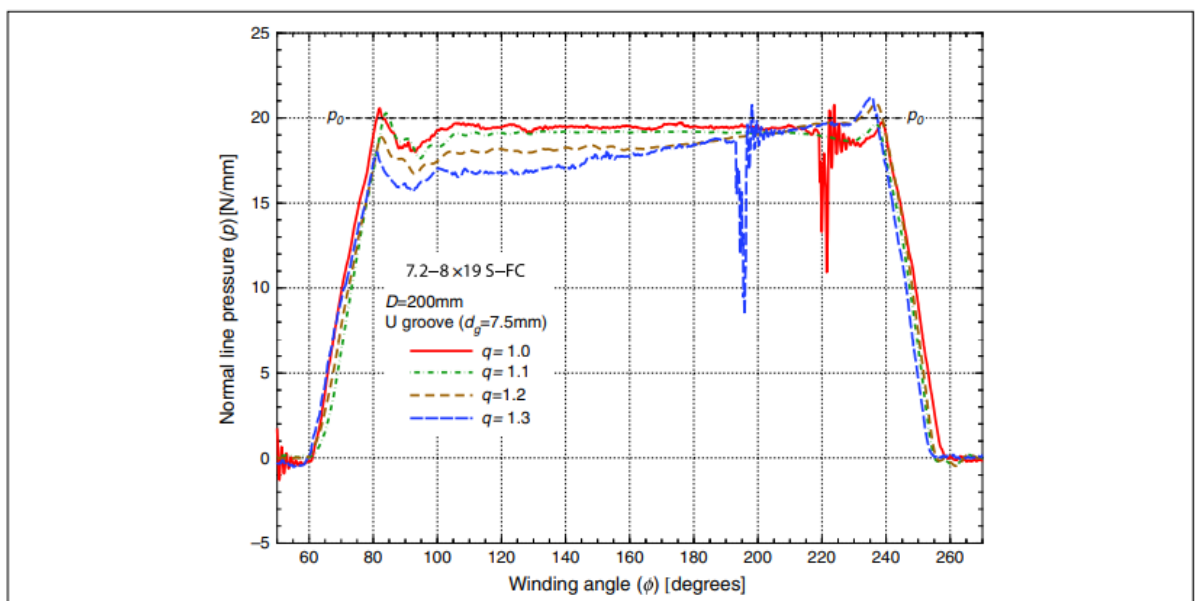


Figure 11. Normal line pressure versus winding angle. (Usabiaga, et al., 2008, p.40)

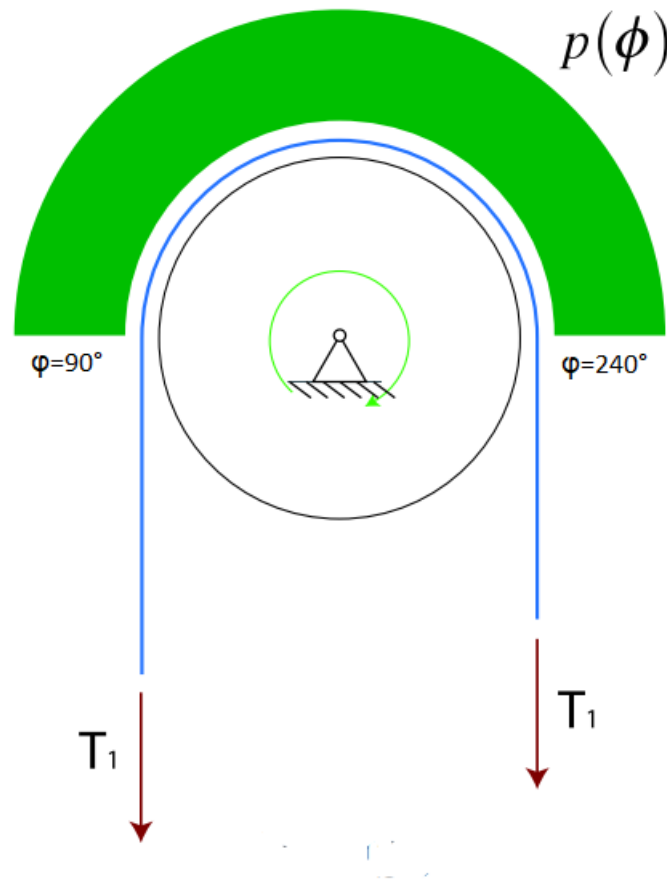


Figure 12. Illustration of sheave showing line pressure and winding angle. (Usabiaga, et al., 2008, p.36)

From figure 11 it can be determined that the contact pressure between rope-off points should be constant. The figure also includes small peaks in both rope off points. This can possibly be explained by friction concentrating on friction sheave.

Research made by Rokita, T. (2016, p.415-424). studies stresses in mine skip hoist sheaves. Sheave design is slightly different than the sheave type studied in this thesis. Sheave studied by Rokita, T. (2016. p.415-424). has single plate web with four holes in it. Stresses in the web should be distributed similarly in any case. The research shows after usage, crack have formed near connection between web and hub. Finite element model shows principal stress is highest near this location. Holes in the web has also small stress concentrations.



Horizontal forces were modelled by simply adding nodal force to the groove bottom on opposite sides in opposite directions. Skew loading model is constrained from fixed constrained in rope ends. Sheave does not have any constraints to allow rotation. Meshing, material model and connection property are identical to other full sheave analysis.

### 3.2. Stresses in sheave cross section

Stresses in the sheave cross section are studied by both 2D finite element models and from 3D finite element models by analysing cut open models. 2D finite element models include analysis of both welded cross section and cast cross section. Welded cross section has similar profile as full model sheave but with shorter webs. Cast cross section has simplified profile form a real cast sheave. Groove and flange profile of both cross sections is identical. Even though the profiles are 2-dimensional they are modelled using 3-dimensional solid elements. Solid elements are used because they made contact between the rope outer surface and groove bottom surface possible. Both models are 1mm thick and z-axis of the cut surfaces are constrained, which leads the model to act in similar way to plane strain elements. Material for both rope and sheave for both models is steel with elastic modulus of  $E = 210\,000\text{MPa}$  and Poisson's ratio of  $\nu_p = 0,3$ . In reality rope has lower elastic modulus in radial direction, but it was found out elastic modulus has a very low effect on stress distribution in the sheave. Element size in both models is 1mm.

Cross sections are constrained from bearing surface. Rope has loading on the upper surface with magnitude of 1000N for welded profile and 500N for cast profile. Magnitude of the stresses is not target of the study, but distribution of them. From rope, the loading is transferred to the sheave by connection. Connection contacts groove bottom surface to the lower half of the rope surface. Contact property is default. Property is the same used in full

sheave analysis which is shown in figure 10. Figure 13 shows welded profile finite element model and figure 14 cast profile finite element model.

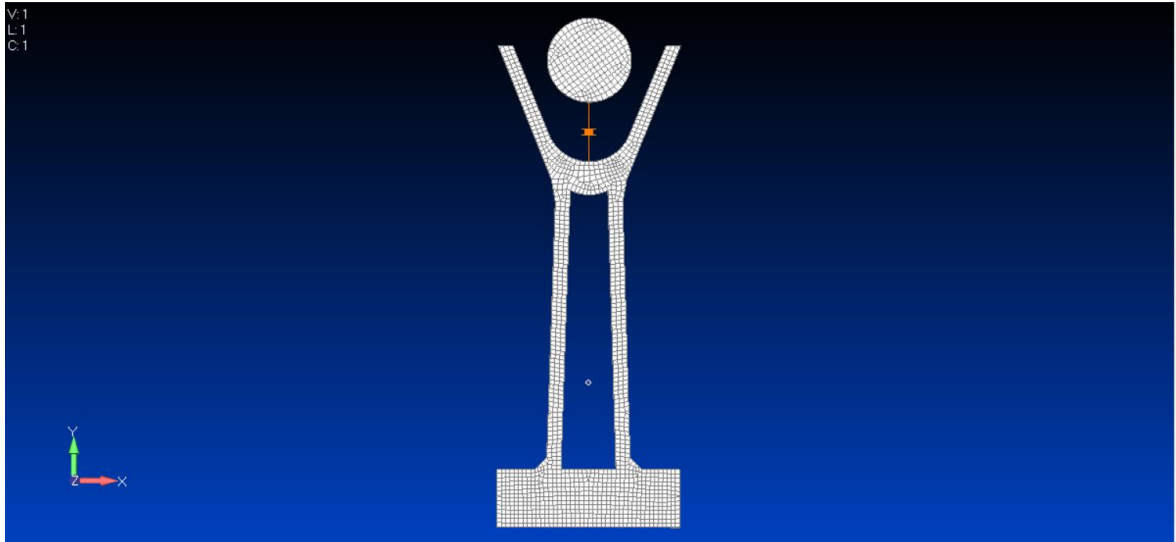


Figure 13. FE-model for the welded sheave cross section. (FEMAP v11.4.2)

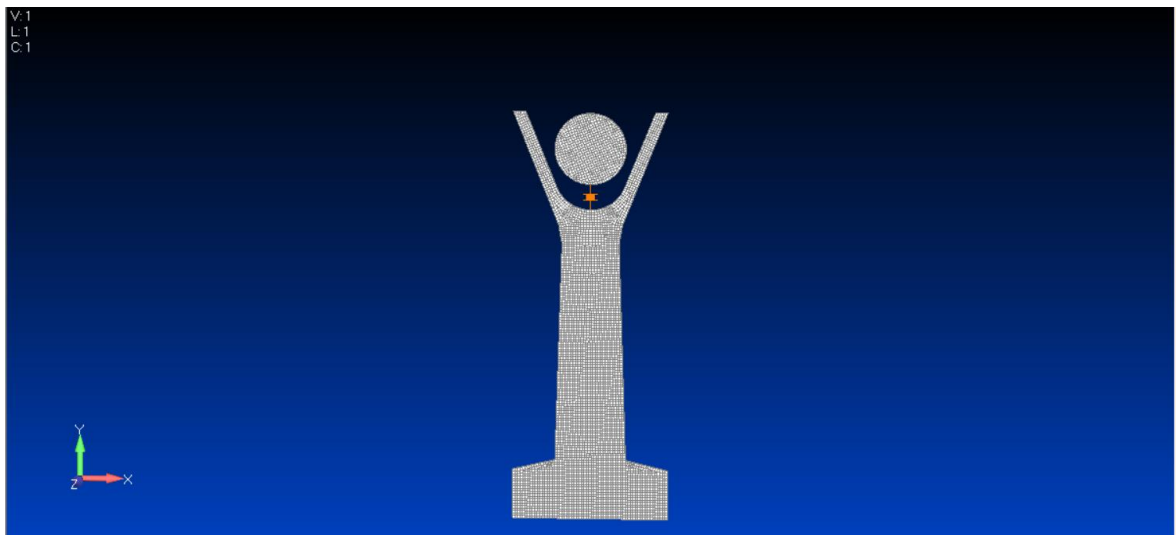


Figure 14. FE-model for the cast sheave cross section. (FEMAP v11.4.2)

2-dimensional finite element models are compared to cut-profiles from full model sheave. Full model sheave is the finite element model from the analysis used to study contact pressure distribution along the groove.

### 3.3. Fatigue analysis using FE-analysis

Effective notch stress (ENS) is a fatigue analysis method for welded joints defined in Hobbacher (2009). In ENS method weld toe and root are replaced with 1mm rounding or hole. Notch stress is obtained from finite element model where weld toes have rounding of 1mm, while hub-web weld root has 1mm hole and weld penetration is replaced with air gap. Notch stress is used to determine fatigue life with regular Woehler S-N-curve. Fatigue class used for calculation is  $FAT = 225\text{MPa}$  for maximum principal stress and slope is  $k = 3$ . Since SFS-EN-13001-3-1 requires fatigue life to be calculated using nominal stress method ENS method can only be used as comparison to it. (SFS-EN-13001-3-1, 2019; Hobbacher, 2009; Hobbacher, 2017, p.807-808)

Figures 15 and 16 show web-hub weld and groove-web weld. Web-groove weld only has smaller mesh in the weld root rounding since it has sharper notch than weld toes. Initially the whole cross section was analysed with 1mm roundings in weld toes and 1mm hole in the roots with air gap between webs and hub. Cross section is otherwise same as analysed in cross section study. Loading is at the groove in y-axis. Cross section is constrained from the hub bottom curve. Elements used in the model were plane strain elements. Initial analysis did not have sub-structures but meshing had smaller size near the roundings.

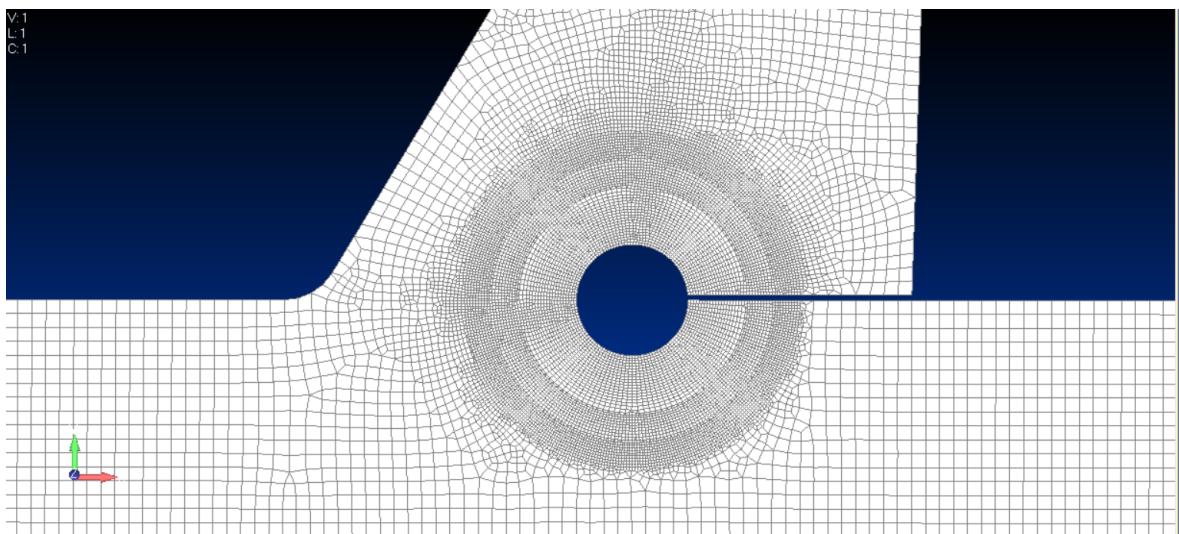


Figure 15. Web-hub weld and its air gap, hole and rounding's. (FEMAP v11.4.2)

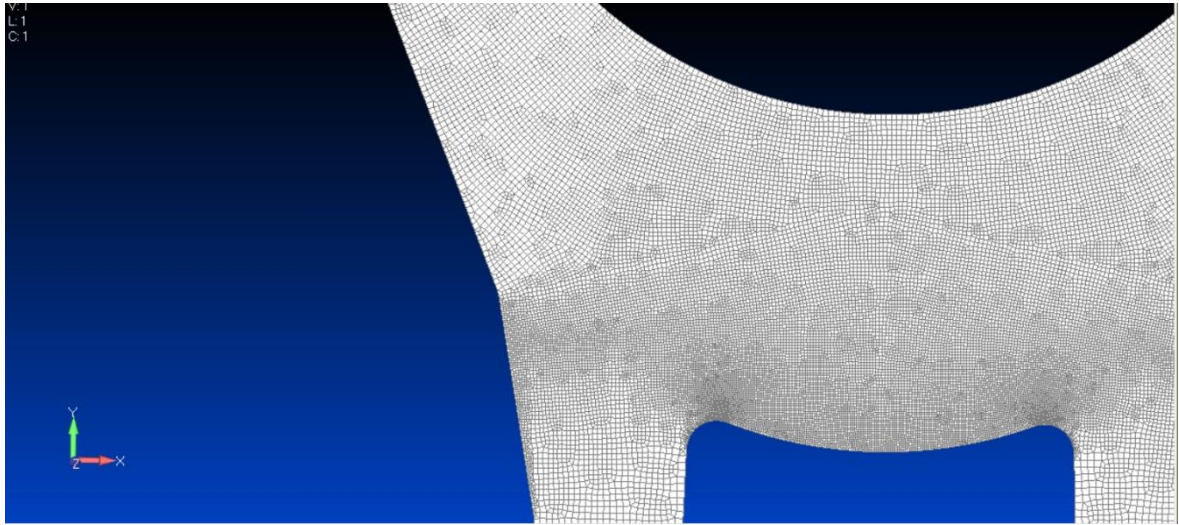


Figure 16. Web-groove weld and rouging's at the weld roots from initial analysis. (FEMAP v11.4.2)

After the full cross section of sheave was analysed, simpler model included only half of hub and other web. Meshing on this model was more accurate around the web-hub weld with sub-structure modelled in the weld root. Element size is 0,05mm on the sub-structure around the weld root. This gives total of 20 elements for the rounding. In rest of the model, element size is 0,2mm. For simplified model translation in x-direction is constrained due to only half of the profile modelled.

## 4. Results and development of the calculation tool

Full finite element model was used to create stress distribution curve along and across the groove length. Cross sectional models were used to study stress distribution rope to critical areas for design. Effective notch stress analysis was used to compare fatigue life to simpler nominal stress method. As cylinder model for rope is not realistic it does not consider very local stresses at the groove accurately. For design, purposes getting average contact pressure distribution is more important. For reliability analysis stresses in welds and the structure are more important. Wear in the groove bottom can be difficult to calculate and it is easier to monitor than fatigue.

### 4.1. Analysis for the pressure distribution along the groove length

Pressure distribution along the groove is used to study locations of maximum stresses and how do those maximum stresses compare to average stresses. Goal is also to study effect of winding angle on the contact pressure distribution. Figure 17 shows Von Mises stress distribution on full model sheave. Highest Von Mises stress can be found near the weld between hub and web. Stresses are distributed symmetrically along Y-axis. Stresses are

significantly larger near the upper part of hub-web weld, which is also shown in research made by Rokita (2016, p.420).

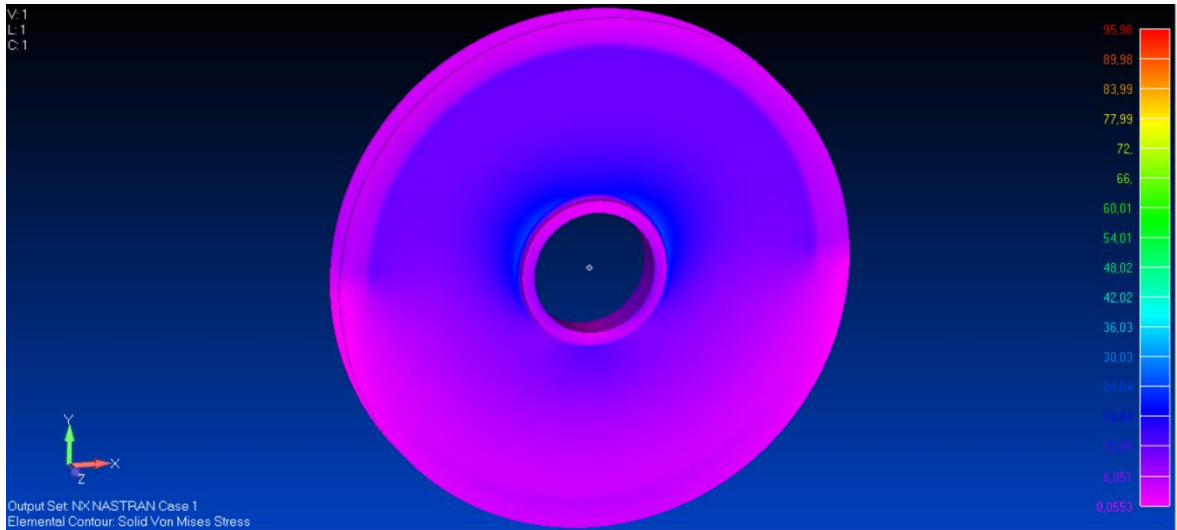


Figure 17. Von Mises stress in the sheave for 180° winding angle. (FEMAP v11.4.2)

Appendix 2 shows Von mises stress distribution in the sheaves for 135° and 90° winding angle. Stress distributions are similar with highest Von Mises stress found near the hub-web connection. Highest stresses can be found between the rope off points, while in the areas without rope connection the stress decreases significantly.

Figure 18 shows contact pressure distribution on the bottom of the groove of FE-analysis for sheave with 180° winding angle. As can be seen from the figure, groove has several discontinuity lines. Pressure distribution is symmetrical along the Z-axis as it should be. Contact pressure in the groove is between 6 MPa – 8 MPa.

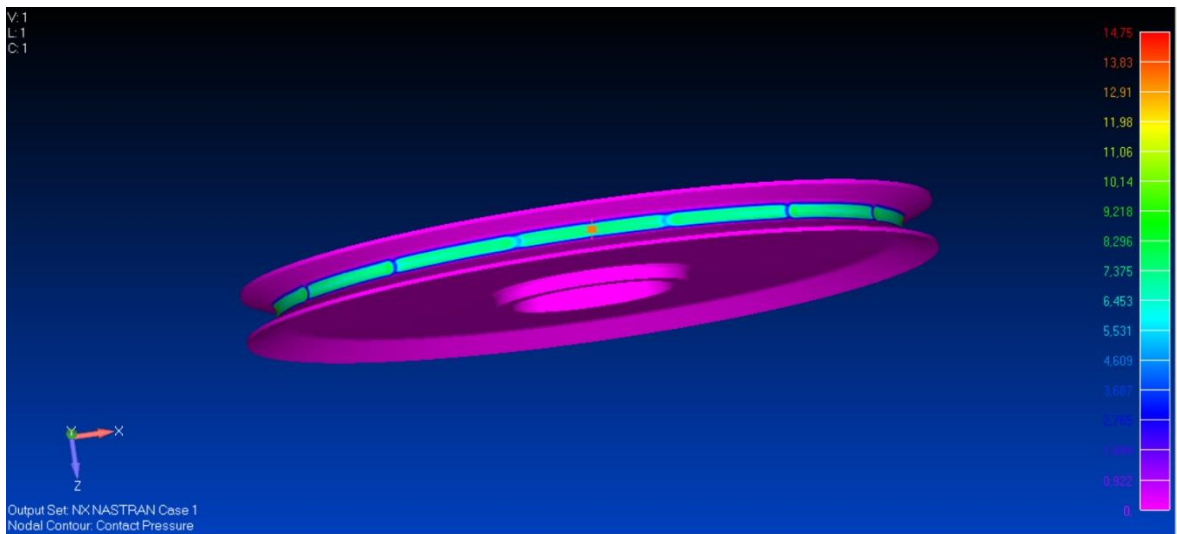


Figure 18. Contact pressure distribution in the groove bottom for 180° winding angle. (FEMAP v11.4.2)

Figure 19 shows contact pressure distribution in the groove of 135° winding angle analysis. Average pressure values for this analysis are slightly higher than for 180° winding angle. Contact pressure without peak is between 6 MPa – 9 MPa. There are discontinuities in similar way as with 180° winding angle. There are 7 peaks total between rope off points. In transverse direction the pressure is smooth.

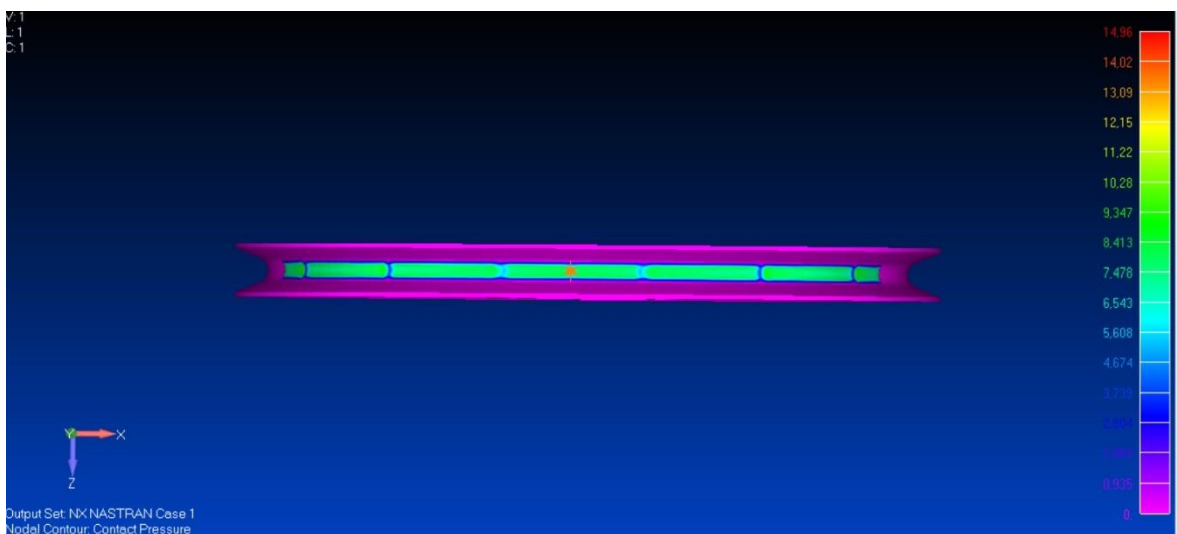


Figure 19. Contact pressure distribution in the groove bottom for 135° winding angle. (FEMAP v11.4.2)

Figure 20 shows contact pressure distribution for 90° winding angle. This analysis has only one discontinuity on each side. Peaks in the rope off point are much greater than with larger angles, while discontinuities in the middle are smallest with 90° winding angle. In transverse direction pressure is distributed smoothly in similar way as with other angles. Between the rope off peak values, contact pressure is between 6 MPa – 11 MPa.

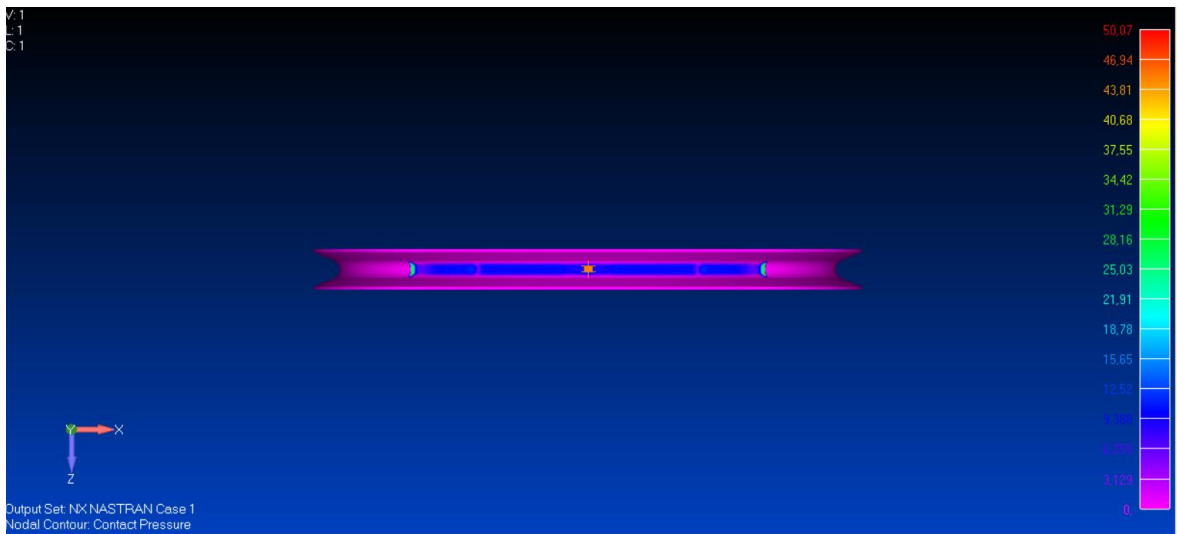


Figure 20. Contact pressure distribution in the groove bottom for 90° winding angle. (FEMAP v11.4.2)

Figure 21 shows contact pressure curve for winding angle of 180°. The curve is made by plotting all the pressure values of nodes in the centre line of the groove. Discontinuities shown in the figure 18 can also be seen in contact pressure curve. Figure 22 shows the same contact pressure curve with discontinuities and peaks filtered. Figure also shows trendline for the curve which is very flat.



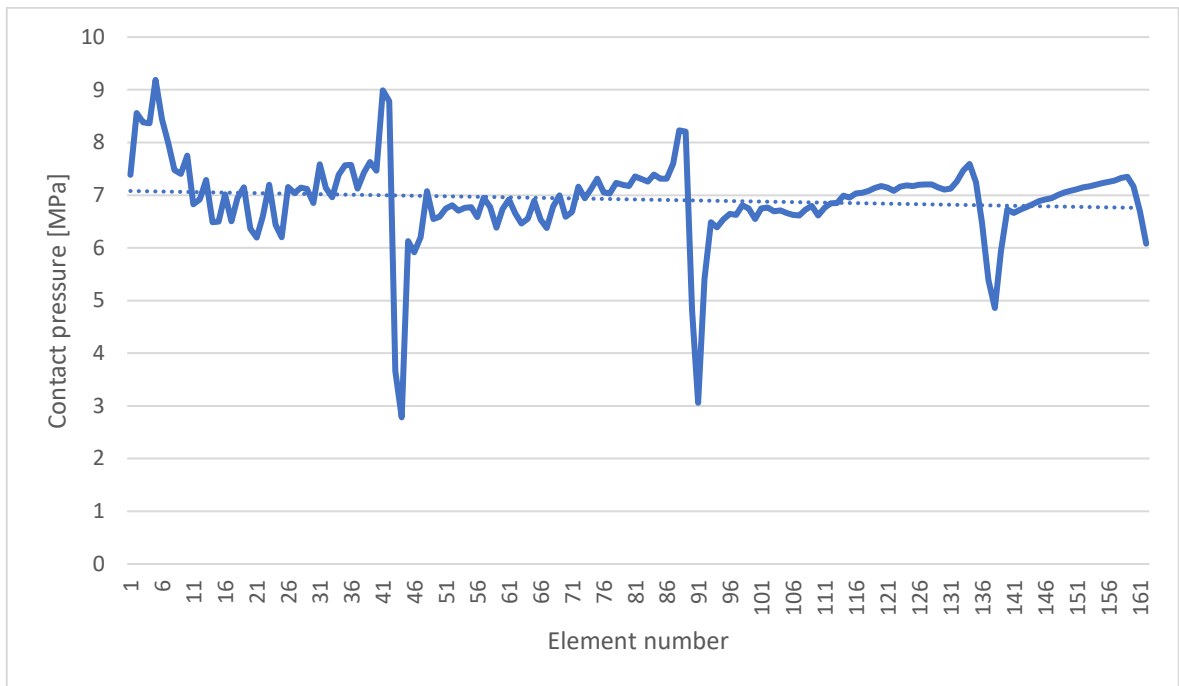


Figure 21. Contact pressure in half groove for 180° winding angle element number 1 being rope off point and element number 162 in the middle.

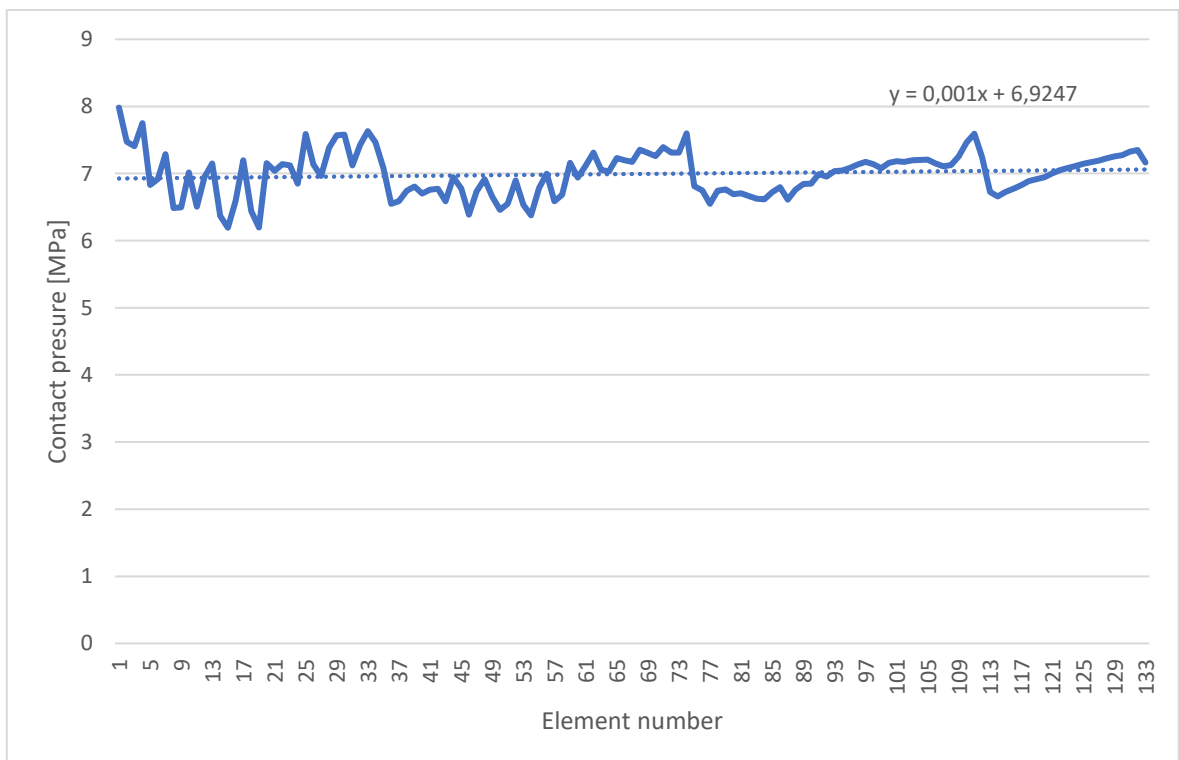


Figure 22. Filtered contact pressure curve in half groove for 180° winding angle element 1 being at the rope off point and element number 133 in the middle.

For winding angles of 135° and 90° contact pressures must be scaled down. Loading on the structure is from the bearing surface. Since 50 kN rope force does not create equal force at the bearing surface, it needs to be scaled by factor of  $\frac{54}{50}$  for 135° winding angle and  $\frac{70,7}{50}$  for 90° winding angle.

Figure 23 shows filtered pressure distribution for contact pressure for 135° winding angle. Figure shows half groove elements, element 1 being in the rope off point and point 97 being in groove middle point. Filtered curve has similar peaks as 180° winding angle curve. Unfiltered curve can be seen in Appendix 3.

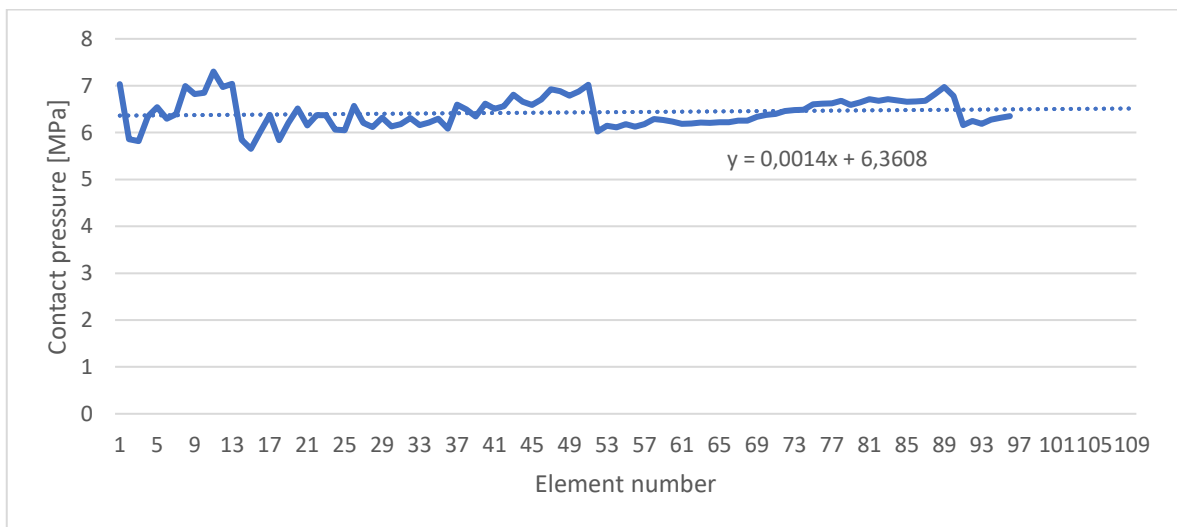


Figure 23. Contact pressure distribution for 135° winding angle.

Figure 24 shows filtered contact pressure distribution curve for 90° winding angle. Unfiltered curve would have peaks in both rope off point and groove middle point. Rope off point had 24 MPa peak value and middle point has 8 MPa peak. Unfiltered curve can be seen in Appendix 4.

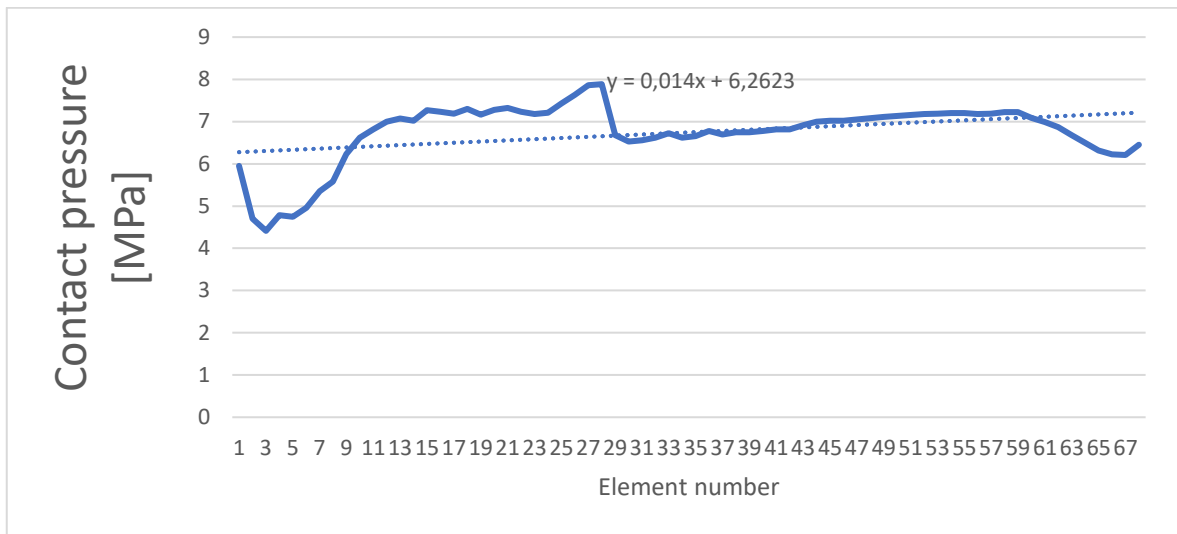


Figure 24. Filtered contact pressure distribution for 90° winding angle.

Filtered curve still has a large drop in pressure near the rope off point and smaller drop in centre line of the sheave, as well as one small discontinuity. Otherwise, the pressure stays fairly smooth.

#### 4.2. Analysis for the pressure distribution along the groove width

Figure 25 shows cross section of welded sheave and figure 26 shows cut open model of similar welded sheave from full 3D-model of a sheave. Both models are modelled using 8-node solid elements. Cross sectional model has in-plane deflection constrained thus it acts like plane strain element. As can be seen from both models, critical locations in the sheave are groove-web weld, web-hub weld and web. The most critical location of the structure is

weld between web and groove. In 2D-cross section Von Mises stress is constant while in full model 3-dimensionality causes stress to increase closer to the web.

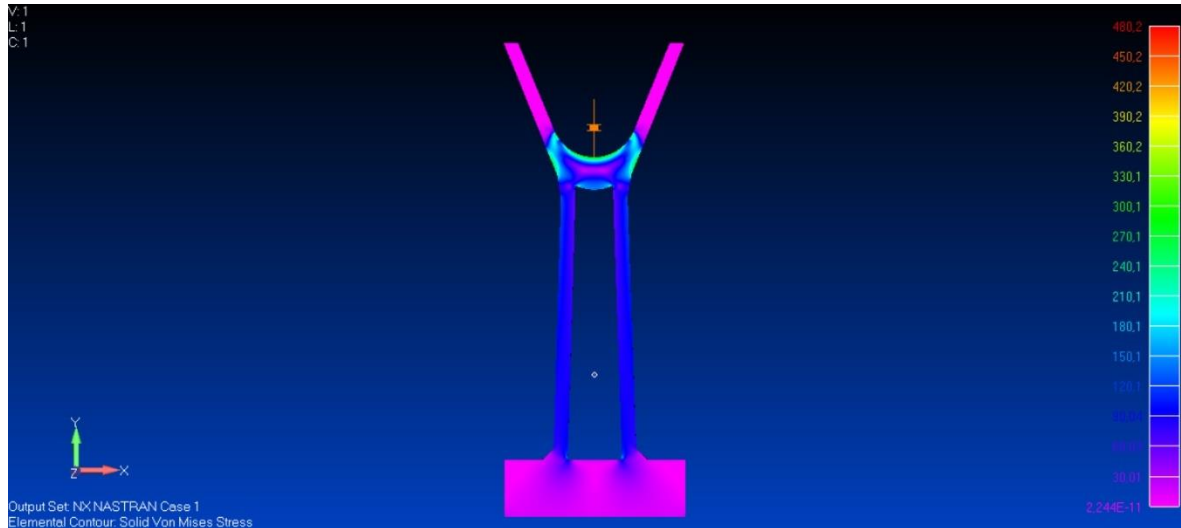


Figure 25. Von Mises stress distribution in welded sheave cross section. (FEMAP v11.4.2)

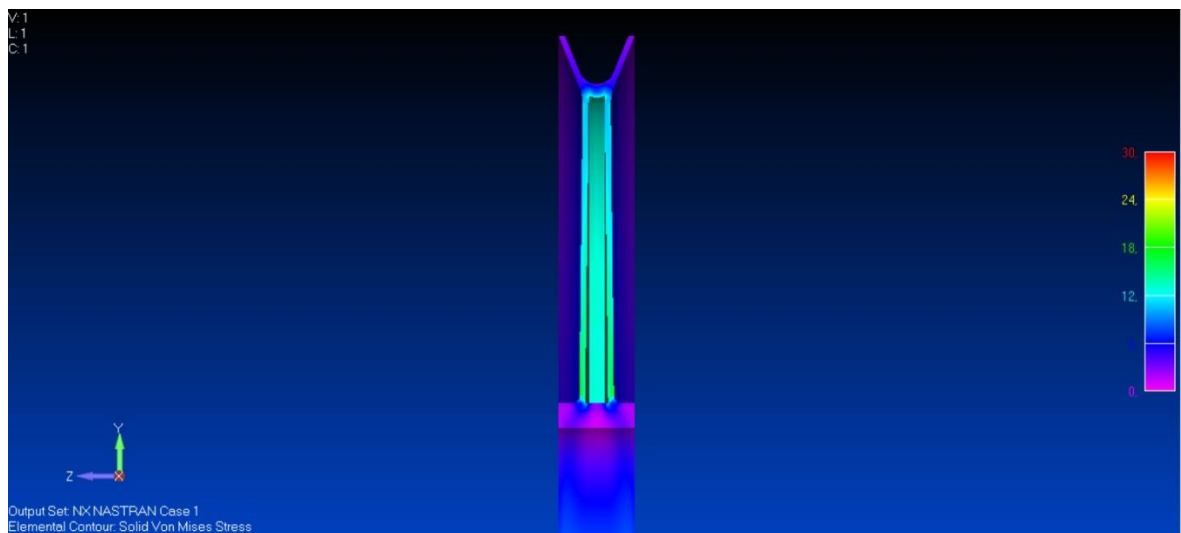


Figure 26. Cut cross section of sheave of full model FE-analysis. (FEMAP v11.4.2)

Figure 27 shows cross section of cast sheave. Like welded cross section, cast one is modelled using 8-node solid elements with in-plane deflection constrained to make the elements act like plane strain elements. As can be seen from the figure, highest stresses can be found from

groove bottom and flange. Stresses in the web are small compared to areas near groove. Possible failure modes according to this FE-analysis are fatigue failure near the flange root or wear in the groove bottom.

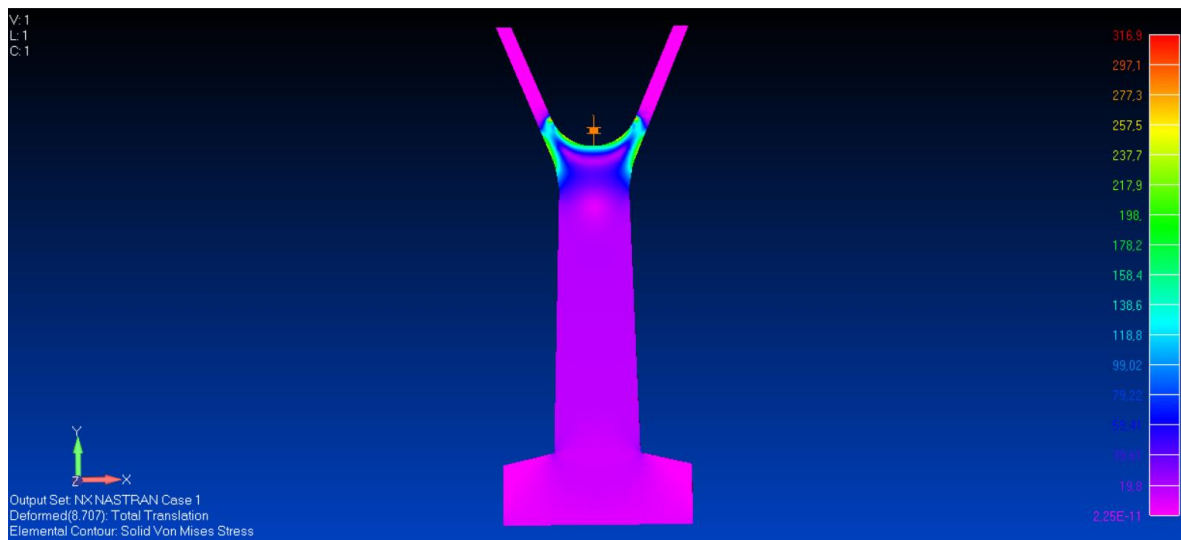


Figure 27. Von Mises stress distribution in cast sheave cross section. (FEMAP v11.4.2)

Figure 29 shows contact pressure in six nodes across the groove bottom. The data is from full model FE-analysis. Mean value of the curve is 5 MPa. Mean contact pressure calculated by equations 19 and 20 give pressure of 5 MPa for 45° groove angle. This shows analytical calculations are accurate enough to be used for sheave design. Figure 28 shows element numbers in groove cross section.

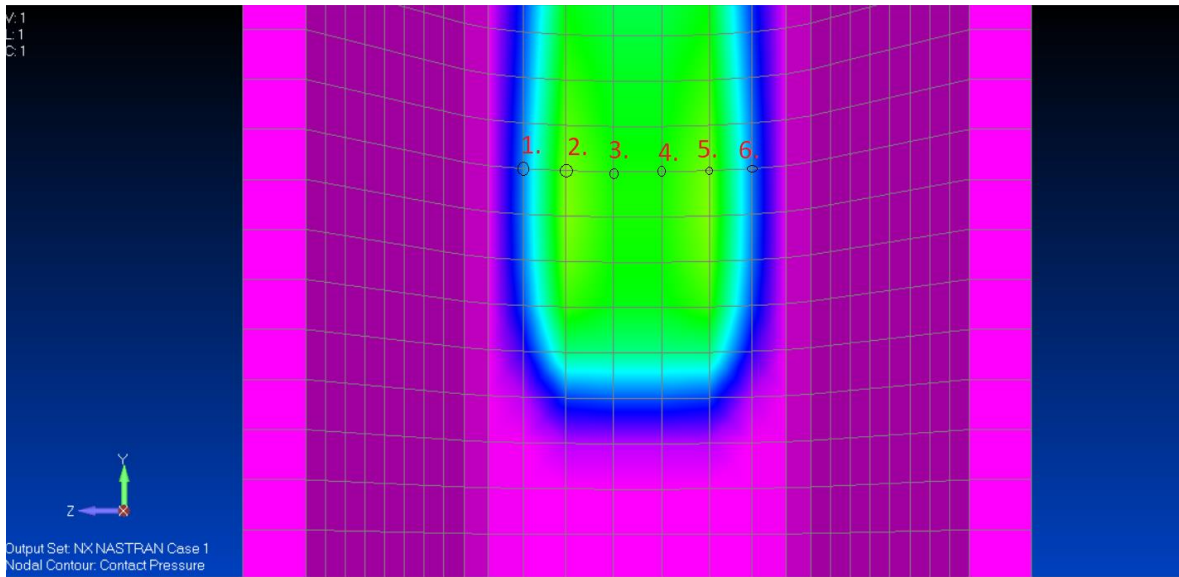


Figure 28. Element numbers in groove cross section.

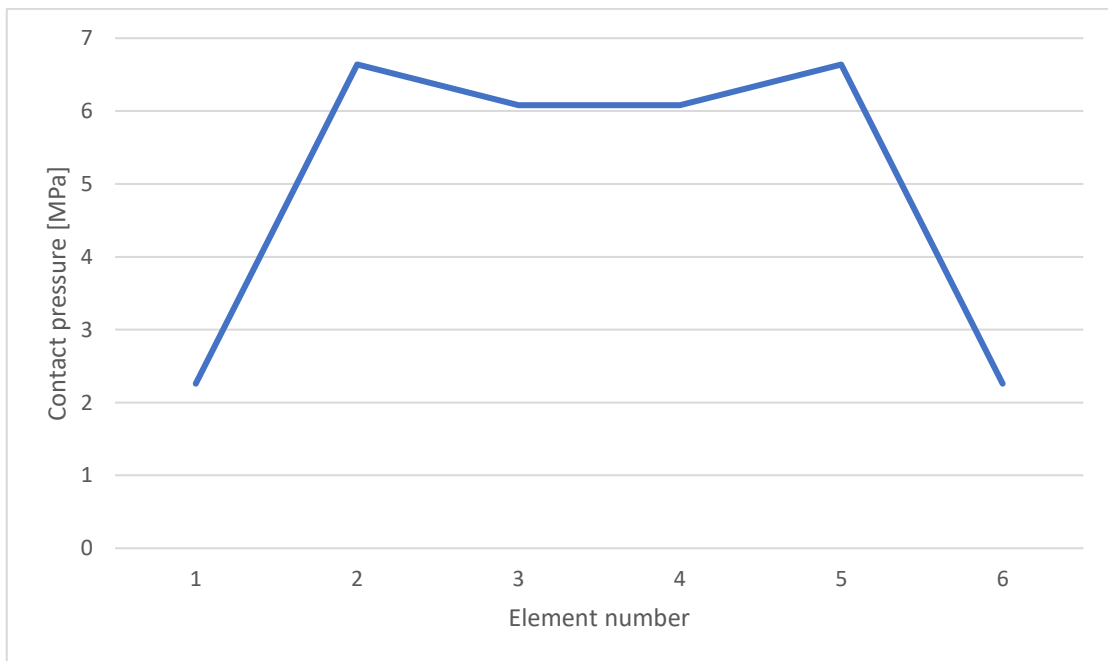


Figure 29. Contact pressure curve across the groove taken from full FE-model for 180° winding angle.

As the figure shows the pressure stays near constant in the groove bottom with while decreasing in the edges. Pressure curve is mirrored from the centre as it should be. Appendix 5 shows same curves for 135° and 90° winding angles.

### 4.3. Horizontal forces

Figure 30 shows deformed view of the model. Deformed view shows rotation of the sheave and large deformation of the rope. Deformation is as it should be. Rope goes through the flange since they do not have contact property between them.

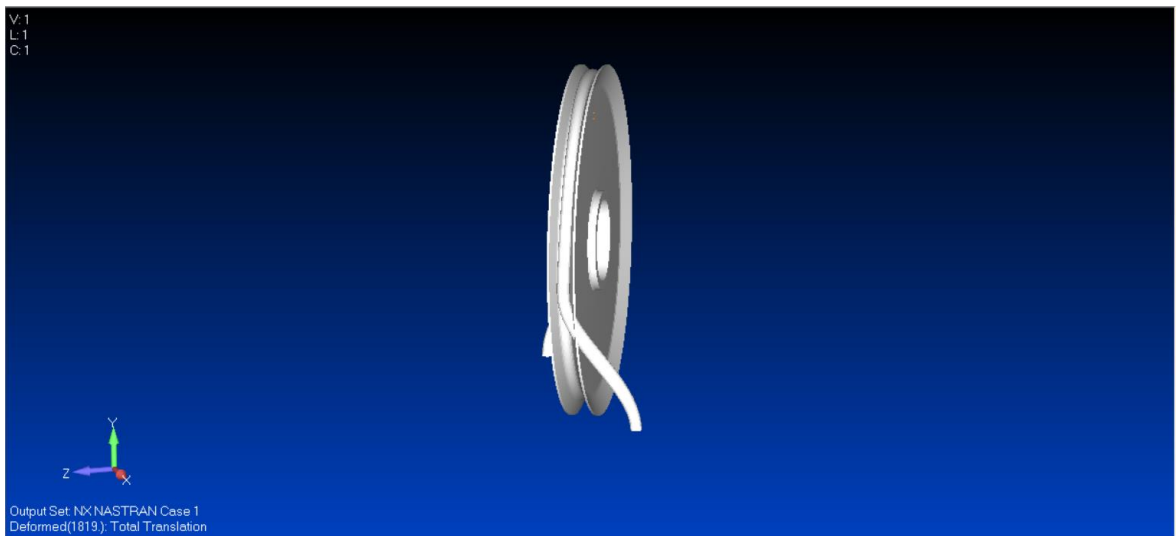


Figure 30. Deformation of horizontally loaded sheave. (FEMAP v11.4.2)

Figure 31 shows contact pressure distribution in the groove. Near the rope off point, the rope starts to climb from the groove bottom as it should be. Otherwise contact pressure is constant along the groove. Skew loading will also create bending moment on the sheave, that leads to larger compression stress on the other web.

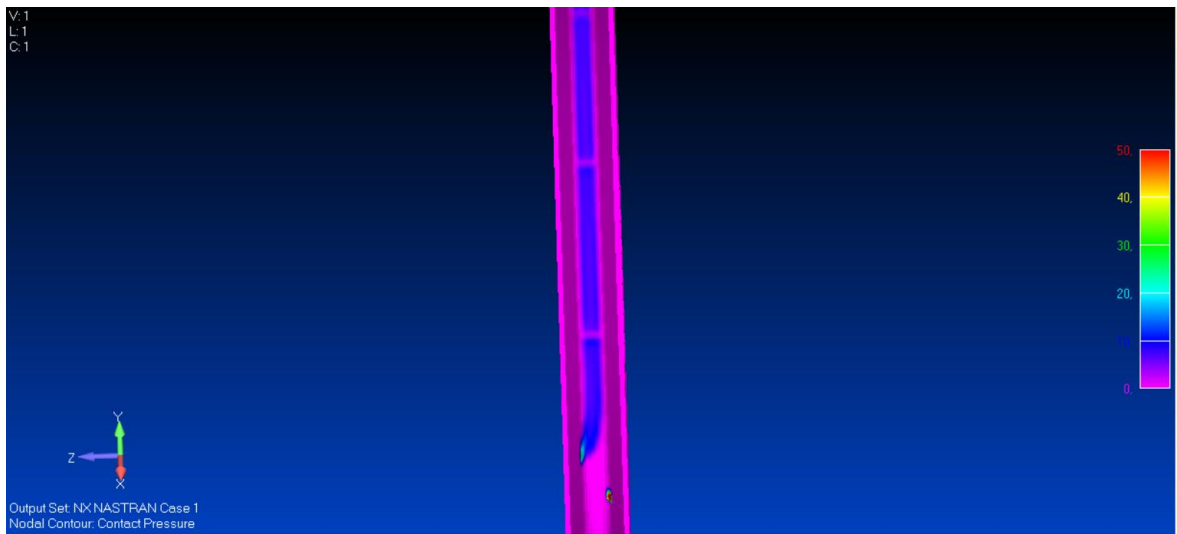


Figure 31. Contact pressure of the horizontally loaded sheave. (FEMAP v11.4.2)

As the figure shows skew loading has small effect on the contact pressure distribution in the groove if the rope stays in the groove. From design point of view skew loading has a large effect on loading in the web which has to be considered in the design.

#### 4.4. Issues in the FE-models of pressure distribution

As can be seen from the figure 32 there are clearly visible discontinuities in the contact pressure of the groove. Contact pressure in the rope has also discontinuities as can be seen from the figure 31. Discontinuities in rope include only peaks, while sheave has both peak



and drop. By switching master-slave surface between the rope and the sheave, discontinuities are also switched.

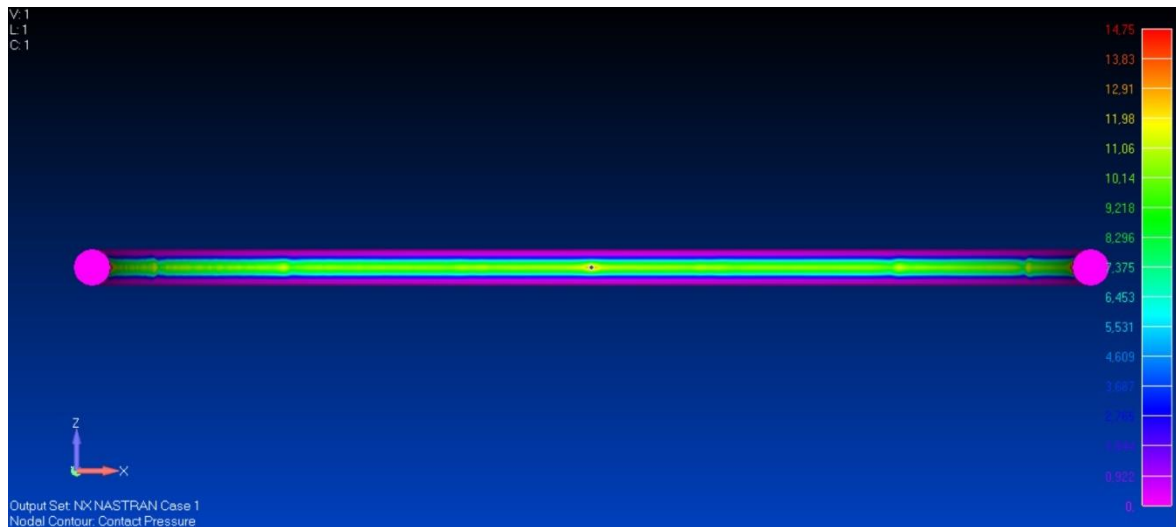


Figure 32. Contact pressure distribution in the rope. (FEMAP v11.4.2)

Possible reasons for discontinuities are meshing, large deformations or issues with contact property. Initially meshing clearly caused issues for calculating contact pressure correctly. Initially mesh size was too high and mesh sizes were different for rope and sheave which led to large amount of random pressure peaks in the sheave. By meshing both with same 4 mm mesh size, most of the discontinuities were eliminated. Analysis with smaller 3mm element size failed. Large deformations will cause elements to stretch which can cause issues for analysis.

Nam-Ho (2015, p.422-423) shows that if contact nodes do not match there can be overpenetration of some nodes and lack of contact for some nodes. Overpenetration could explain random pressure peaks with coarse meshing rope and unmatched meshes. Discontinuities in the final model could not be explained by overpenetration and lack of contact, since mesh size equals for both bodies, discontinuities are not random, and they are not sharp.

Figure 33 shows groove bottom with master-slave surfaces switched. As the sheave should be the master surface and rope the surface, it was tested what kind of effect does the surface

modes have on the contact pressure. From the original analysis it could be seen that pressure distributions in the rope and the sheave are not identical.

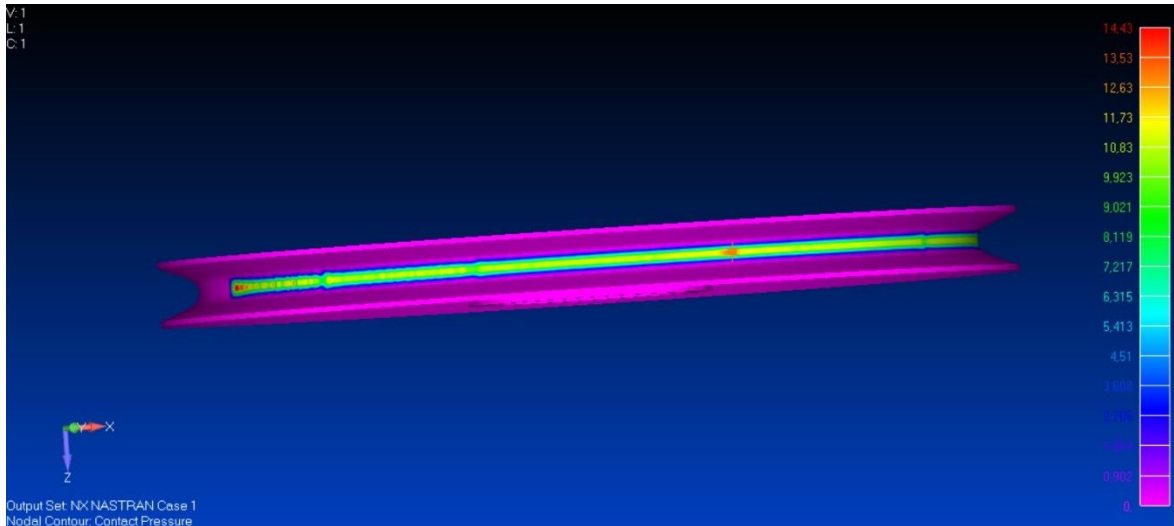


Figure 33. Contact pressure in the sheave with contacts master-slave surfaces switched. (FEMAP v11.4.2)

If master-slave surfaces are switched, contact area decreases in transverse direction, rope off points have many pressure peaks and there are still discontinuities in the groove. Contact pressure has also higher maximum value, compared to master-slave surfaces other way. Discontinuities could not be eliminated by making both surfaces' masters and slaves as suggested by Nam-Ho (2015, p.418).

Initially only upper half of the sheave was modelled with symmetry constraints. Modelling only the upper half led to large pressure peaks in the rope off points. Initially the rope was also modelled without any extensions, which led to similar pressure peaks in the rope off point. Only downside from using full sheave and rope extensions was larger number of elements, which did not have a large effect on computation time, since non-linear connection determines most of it.

## 4.5. Developing the calculation tool

Purpose of studying contact pressure distribution, cross section and fatigue is to create a reliable way to design a sheave. As the contact pressure is not constant in transverse direction maximum contact pressure along the groove width must be considered.

The standard before SFS-EN-13001 was FEM 1.001 3<sup>rd</sup> edition Booklet 3 and Booklet 4. Design of sheaves is defined in FEM 1.001 3<sup>rd</sup> edition booklet 4. (p.19-21). This standard defines minimum winding diameter and minimum groove diameter, as well as defines safety factors. Nothing more is demanded in this standard. FEM 1.001 3<sup>rd</sup> edition booklet 3. defines material selection and elastic limit states for cranes. SFS-EN-13001-3-3 is a standard for competence of wheel/rail contact. Maximum contact pressure for static and fatigue cases are defined in the standard. Contact type between a wheel and a rail is not like contact between a sheave and a rope, thus equations for calculating limit contact force are not useful for this case. Wear in these cases is not similar either. For wheel/rail contact, pitting and surface cracking are the expected wear typed and for sheave/rope contact it is abrasive wear caused by deformation of rope. (SFS-EN-13001-3-3, p.1-18)

### 4.5.1. Contact pressure

Mean contact pressures along the groove length and width, as well as calculated contact pressures for different winding angles are listed in table 1. Longitudinal pressure values in the table are mean values of the pressures along the centre line. Transverse pressures are mean stresses from top point of the sheave. As the table 1. shows contact pressure does is not affected by winding angle of the rope.

Table 1. Average contact pressures.

Winding angle	Longitudinal [MPa]	Transverse [MPa]	Equation 19 [MPa]	Equation 20 [MPa]
180°	6,9	5,0	5,6	5,6
135°	6,4	5,0	5,6	5,6

90°	6,3	6,4	5,6	5,6
-----	-----	-----	-----	-----

EN-13001-3-2 defines two factor that can be directly used as factors for calculating contact pressure. Figure 34 shows how values are measured from a groove. Figure 35 shows corresponding  $f_{f6}$  factor for each  $\frac{r_g}{d}$  value. Calculated contact pressure should be divided by factor  $f_{f6}$ . (SFS-EN-13001-3-2, 2014, p.25)

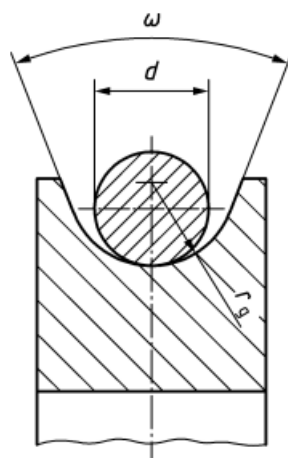


Figure 34. Groove dimensions. (SFS-EN-13001-3-2, 2014, p.25)

$\frac{r_g}{d}$	$\omega$	$f_{f6}$
0,53	$\leq 60^\circ$	1
0,55		0,92
0,6	No requirement	0,86
0,7		0,79
0,8		0,76
$\geq 1,0$		0,73
Intermediate values may be interpolated.		

Figure 35. Factor  $f_{f6}$  for  $\frac{r_g}{d}$  values. (SFS-EN-13001-3-2, 2014, p.25)

Rope type can be considered by factor  $f_{f7}$  which is calculated by:  $f_{f7} = \frac{1}{t}$ , where  $t$  is the rope type. List of  $t$ -factor is in figure 36. Calculated contact pressure is also divided by factor  $f_{f7}$ .

Rope type in accordance with EN 12385-2	Number of outer strands	$t$ -factor
Single layer or parallel-closed	3	1,25
	4, 5	1,15
	6 or more	1,00
	6 to 10 with plastic impregnation	0,95
Rotation-resistant and non-compacted	all	1,00
Rotation-resistant, compacted	all	0,9

Figure 36.  $t$ -factor for different types of ropes, (SFS-EN-13001-3-2, p.26)

Table 2 shows examples of allowable contact pressures for sheave made of manganese steel. These values are only examples and should not be used as strict limits, since manganese steel is only one type of material. These contact pressure values are clearly below yield stress of any steel. For cast iron and carbon steel cast sheaves contact pressure values are even lower. Low values for contact pressure are to avoid excessive wear. (American iron and steel institute, 1979, p.37-43)

Table 2. Suggested maximum contact pressures for manganese steel sheave for regular lay type of ropes. (American iron and steel institute, 1979, p.38)

	6 × 7	6 × 19	6 × 37	8 × 19
Contact pressure	10 MPa	17 MPa	21 MPa	24 MPa

Table 3 shows suggested maximum contact pressures for manganese steel sheave for lang lay type of ropes. As can be seen lang lay type of rope can be used with higher contact pressures. Allowed contact pressure also increases as number of wires and strands in the rope is increased higher contact pressures are allowed. This is because of higher wear surface in the rope with ropes that have higher number of wires and strands. Wear of the sheave is caused by expansions of the rope which leads to rubbing. Table 4 shows suggested maximum contact pressure values for sheaves made of cast iron and carbon steel castings. Values from tables 3 and 4 should be considered as suggestions. Both cast irons and carbon steels include wide range of materials with large variation of properties that have a great influence on contact pressure they can bear without excessive wear. Rates of wear at the maximum contact pressures are not known. (American iron and steel institute, 1979, p.37-43)

Table 3. Suggested maximum contact pressures for manganese steel sheave for lang lay type of ropes. (American iron and steel institute, 1979, p.38)

	6 × 7	6 × 19	6 × 37	Flattened strand lang lay
Contact pressure	11 MPa	19 MPa	23 MPa	28 MPa

Table 4. Suggested maximum contact pressures for cast iron and carbon steel cast sheave for lang lay type of ropes. (American iron and steel institute, 1979, p.38)

	6 × 7	6 × 19	6 × 37	Flattened strand lang lay
Cast iron	2 MPa	4 MPa	5 MPa	6 MPa
Carbon steel cast	4 MPa	7 MPa	8 MPa	10 MPa

#### 4.6. Fatigue analysis

Fatigue analysis of the sheave is done using nominal stress method according to SFS-EN-13001-3-1. 2-D cross section of the sheave was used to compare nominal stress method to ENS (Effective notch stress). From the early analysis without accurate mesh in the sub-structure, it was noticed that highest notch stress can be found from root side of web-hub weld. Thus, simplified model was meshed with more accurate mesh around the area. Figure 37 shows mesh and Von Mises stress around the root rounding. Figure 38 shows the whole simplified cross section.

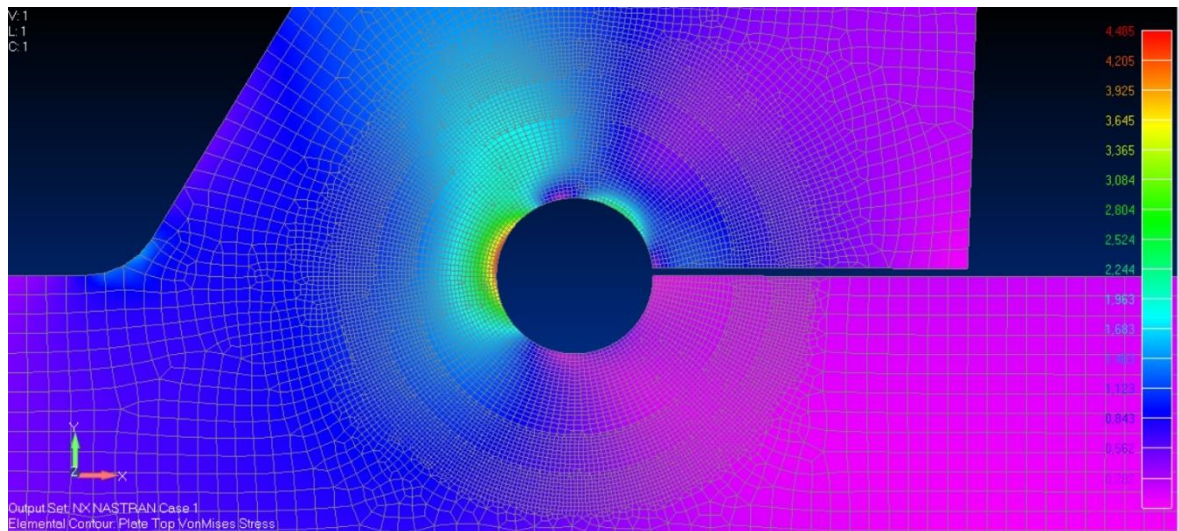


Figure 37. Notch stress at the weld root of web-hub joint. (FEMAP v11.4.2)

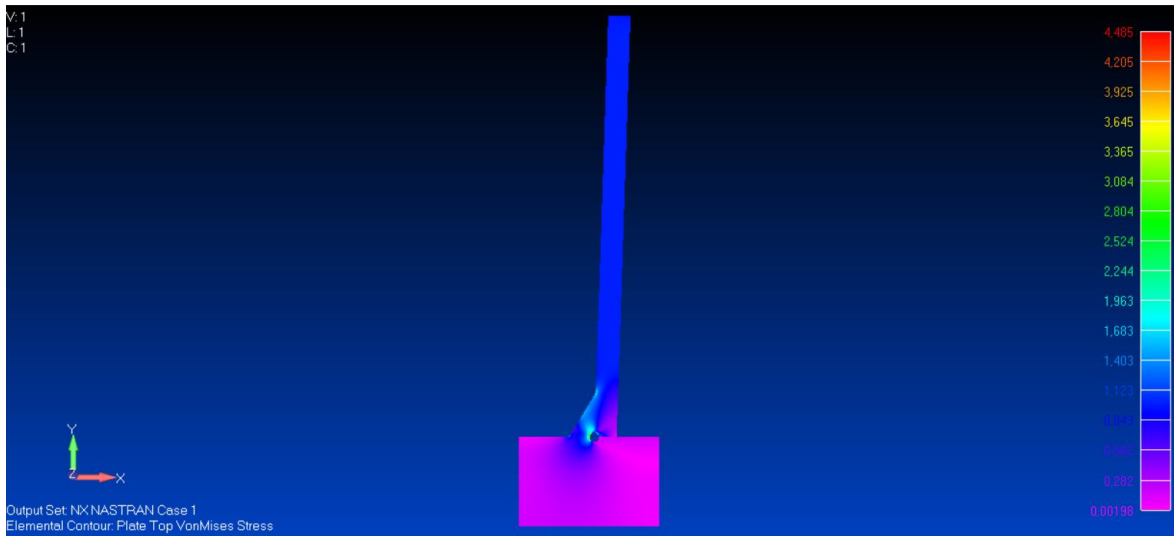


Figure 38. Simplified cross section for ENS-analysis. (FEMAP v11.4.2)

$$\Delta\sigma_{Rd} = \frac{\Delta\sigma_c}{\gamma_{mf} \sqrt[3]{S_m}} \quad (21)$$

Equation 21 is equation used to calculate design limit stress of a detail according to SFS-EN-13001-3-1 (p.147). Notch factor is obtained by dividing Von Mises stress at the notch by Von Mises stress at the web. Notch factor at the root is  $K_t = 4,5$ . Von Mises stress can be used since normal stress is great compared to shear stress. Using this value to calculate design limit stress by equation 21 gives design limit stress  $\sigma_{Rd} = 89$  MPa. In comparison using fatigue class of 71 MPa and equation 21 gives design limit stress of  $\sigma_{Rd} = 124$  MPa for the same detail. Higher value from the nominal stress method is caused by the construction detail not being perfectly suitable for the weld in sheave. In sheave, angle of the web will lead to bending stress in the weld. Bending stress in T-joint will have fatigue class of 45 MPa, 71 MPa or 80 MPa. This detail has number 3.10 from SFS-EN-13001-3-1. p.174. Calculating design limit stress using fatigue class of 45 MPa gives value of  $\sigma_{Rd} = 78,6$  MPa. This is far below results of ENS analysis and can not be used as it is.

The most critical joint for a sheave is the weld between hub and web. For 800 mm sheave with flange width of 10 mm, rope force of 200 kN and cycle number of 1 920 000 cycles. Cycle numbers are calculated from sheave and rope system dimensions and expected number



work cycles. Design stress for these calculations gives design stress value of 83 MPa. Example sheave is expected to withstand its expected lifetime. Typically sheave positions are changed in rope system over lifetime to share fatigue loading and wear more equally. This is caused by different sheaves rotating with different speeds based on their location on the rope system. Position changes should be mandated to be considered in calculations.

Effect of skew loading can be considered by taking it into account in fatigue loading. In lifetime of a sheave skew loading can be considered to even out. According to SFS-EN-13001-3-2 (p.24) maximum allowed fleet angle is  $4^\circ$ . Calculating effect of skew loading is not necessary since it plays small role and predicting skew loading scenarios is difficult.

## 5. Conclusions and evaluation

Purpose of this study was to study contact pressure distribution and stress distributions of a sheave to create a calculation tool to dimension sheaves according to SFS-EN-13001. This goal was achieved. Stress distribution along and across the groove were studied, stress distributions in the structure were studied and ENS-analysis was done for welds. By studying contact pressure and stress distributions contact forces can be modelled correctly in the calculation tool. ENS-analysis confirmed results of nominal stress method from SFS-EN-13001, even if the structural detail was more complex than initially expected.

Expected results of the research are that the contact pressure is mostly constant along the groove length. Average contact pressure should be close to the calculated contact pressure from previous research. Von Mises stress in the sheave structure should have the highest value near the hub connection. Longitudinal pressure from the analysis is close to constant for 180° winding angle. Smaller angles are less constant. Average contact pressure from FE-analysis is close to the calculated one for 180° winding angle. For smaller winding angles contact pressure remains the same. Von Mises stress in the structure is similar than the previous research predicts.

Although issues relating to contact pressure in the groove could not be completely solved, contact pressure distribution curves could be used as basis for calculation tool. Main issue with contact pressure was discontinuities in both sheave and rope. From distribution curve it was determined that contact pressure distribution is constant in the sheave. This result correlates with research made by Usabiaga et. al (2008), which shows constant contact pressure with minor peaks in the rope off point. This study did not have similar peaks in rope off point which is explained by lower friction in this type of sheave.

Most practical issues relating to finite element model could be solved. Modelling rope realistically was difficult task since rope has high elastic modulus in axial and radial direction but low bending resistance. Low bending resistance is the most important property; thus, the rope was modelled by the material having very low modulus of elasticity. Modulus of elasticity being unrealistically in axial and radial direction is not a large issue since contact forces are same in size with same distribution. Issue by having low modulus of elasticity is large deformations as the rope had in this case. Possibility of large deformations causing

discontinuities in contact pressure was thought but none of the contact node pairs went inactive, even with low search distance. Contact pressure of the FE-analysis was confirmed by analytical calculation that were same magnitude. Line pressure was calculated by equation 18, which was divided by area of the groove. To fully confirm the results, practical experiment should be made where a real sheave would be loaded, and stresses measured.

2-dimensional model did not work as intended. Difference in stress distributions in cut open model and 2-D finite element models was great. 2-D finite element models have the highest Von Mises stresses in the groove and in the structures near the groove-web weld. For cut open model highest stress can be found in the web. Calculating contact pressure by equation 20 shows and normal stress in the web by static equations shows the highest stress should be in the web. As diameter of the sheave decreases towards the hub, stress should increase towards the hub. Cut open model shows this clearly, but 2D-model does not, since it does not consider increase in diameter of the cross section.

Effective notch stress analysis was successful. Bending stress in the web has higher effect on the notch factor than initially expected. This shows the fatigue class of just the normal loading cannot be used.

Calculation tool for sheave was created using results of FE-analysis and standards SFS-EN 13001-3-1 and SFS-EN 13001-3-2. Finite element study shows contact pressure stays constant along a groove. Contact pressure remains constant regarding the winding angle. Constant pressure along length of the groove makes calculation simpler.

Research has both novelty value and usability. Even though there is previous research about stress distribution in sheaves they are different types of sheaves, and no research was available for this type of sheave. FE-analysis shows the stresses are low even with realistic loading, while wear and corrosion can be high. Wear and corrosion being prevalent failure modes might be the reason for lack of research about stresses in sheaves. Thesis can be used to design sheaves, so the results can be considered useful.

### 5.1. Reliability and validity of the study

The largest limitation of this thesis is that it does not use triangulation method and only quantitative experiment was finite element analysis, which is only an approximation. By doing experimental test on a sheave, results could be verified. For this thesis, practical experiment was not possible, due to time constraint. To increase reliability experimental results should be compared to results of this research. Practical experiment could be a study using strain gauges near the welds and on the web. Research methods were valid for analysing contact pressure and stresses in sheave. Using these results a sheave can be dimensioned as was goal of the research. Previous research and textbooks suggest that the research is reliable, thus it can be used as a basis for dimensioning.

### 5.2. Further studies

Stress distribution in groove could be further studied by using realistic model for the rope. Since rope is a complex shape comprised from small strands, the model would have a very high number of elements. Realistic model for the rope would eliminate issues about material properties in this thesis. Defining contact surfaces from the rope would create new issues on the other hand. To make the study more valid different kinds of ropes should be studied. Large number of elements, complex connection, difficult modelling and large number of different types of ropes would make computation time of the analysis and the study in general long. An example how a rope should be modelled is shown in research made by Guifang. et. al. (2020. p.1-13). Rope could be modelled with anisotropic material model where elastic modulus is low but elastic modulus is realistic in radial dimension. This type of material model was not used in this research since it is expected to have small effect on pressure distribution along the groove length. Welds can be analysed further by using linear elastic fracture mechanics method.

The best way to increase lifespan of a sheave would be to minimize wear. Future research could focus on how to minimize wear of both sheave and rope, and what should be the relation of hardness between sheave and rope. Studying wear of sheaves is difficult, since

there are many types of wear, like abrasive wear and surface fatigue, as well as corrosion. Rope surface quality's effect on surface pressure, wear and fatigue of both components.

Studies on sheaves should continue by studying effects of the material. Sheaves can also be made from cast iron or nowadays also from fibre reinforced polymers. Sheaves made from these materials have different cross sections than welded steel sheaves. Polymer sheaves also have very different material properties that influence the design. Since there are large number of reinforcement and matrix materials there should be a comprehensive study made what kind of combinations could be used on sheaves.

Real life study how factors in SFS-EN-13001-3-2 represent real life situations. By studying how these factors function, more accurate input data can be used in design. Also, real life study could focus on studying order of sheaves in rope systems and how the orientation and changing it can affect loading, wear and service life in general.

## 6. Summary

This thesis studied contact between rope and a sheave, stress distribution within a sheave and fatigue of the welds in a sheave. The goal was to find numerical factors for maximum and average contact pressure between sheave and rope, factors for effect of winding angle on contact pressure, confirm magnitude and locations of maximum stress values in the web and welds, and compare nominal stress method and effective notch stress method in assessing fatigue life of the welds. Stress and contact distributions were studied using FE-analysis. Fatigue life was studied using ENS method by FE-analysis. In literature review standard SFS-EN-13001-3-1 was studied to prove strength of the structure and welds. SFS-EN-13001-3-2 was studied to find factors that can be used to assess loading on a sheave.

Result of the contact pressure study was that, contact pressure remains constant along the longitudinal direction of the groove, while in transverse direction it has decreases at the edges, while staying constant in the middle of the groove. Winding angle has no effect on the contact pressure. Size of the sheave, rope and opening angle influences the pressure, as literature suggests. Maximum Von Mises stresses can be found near web-hub connection, as previous research suggests. ENS-analysis confirmed results of nominal stress method. Fatigue analysis of a typical sheave shows that welds can withstand expected loading for a lifetime. By changing position of a sheave in rope system, number of rotations can be changed. By switching positions fatigue loading can be spread more evenly among sheaves. Issues with discontinuities in the pressure distribution, that can be caused by large deformation or curvature of the contact elements, could not be eliminated from the analysis. To reach desired reliability of the results, practical experiments on a sheave should be made. Results can be considered reliable enough anyway. Results can be used in developing a calculation tool for sheaves.

Thesis shows the future research should focus on studying wear of the groove. This can be done by doing more accurate FE-analysis of the contact. Effect of hardness and corrosion should be studied as well. Wider study about use of SFS-EN-13001-3-2 in design of sheave would be interesting and useful as well.

## References

American iron and steel institute. (1979). Wire rope user's manual. Washington, D.C., USA.  
American iron and steel institute. p.5-126

Budynas. R. G., Nisbett. J. K., (2011). Shigley's mechanical design. 9<sup>th</sup> edition. USA.  
McGraw-Hill. p.919

Certex Finland Oy. (2022). Technical description. [referenced on 13.5.2022]. Available:  
<https://www.certex.fi/en/technical-info/steel-wire-rope/technical-description>

Federation Europeenne de la manutention. (1998). Rules for the design of hoisting  
appliances: Booklet 3: Calculating the stresses in structures. 1.001 3<sup>rd</sup> edition. Helsinki:  
Federation of Finnish metal, engineering and electrotechnical industries

Federation Europeenne de la manutention. (1998). Rules for the design of hoisting  
appliances: Booklet 4: Checking for fatigue and choice of mechanism components. 1.001 3<sup>rd</sup>  
edition. Helsinki: Federation of Finnish metal, engineering and electrotechnical industries

Gosan. (2022). Product catalogue: Sheaves. [referenced on 13.5.2022]. Available:  
<https://gosan.net/wp-content/uploads/2021/05/SHEAVES.pdf>

Guifang, H., Chunfu, S., Hongwei, H., Rong, Z., Ding, Y., Xin, N., Fanggang, N., (2020).  
Mathematical and geometrical modelling of braided ropes bent over a sheave. Journal of  
engineered fibers and fabrics. Vol.15. p.1-15

Hobbacher, A.F., (2017). Comparison of fatigue verification procedures at a thick-walled welded component. *Welding in the world*. Vol.61 (4). p.801-818

Hobbacher, A.F., (2009). The new IIW recommendations for fatigue assessment of welded joints and components – A comprehensive code recently updated. *International journal of fatigue*. Vol.31 (1). p.50-58

Nam-Ho. K., (2015). *Introduction to nonlinear finite element analysis*. Boston, MA. Springer ebooks

Rokita. T., (2016). Tests and examination of drive sheave in mine skip hoist. *Archives of mining sciences = Archiwum górnictwa*, Vol.61 (2). p.415-424

SFS-EN-13001-1. (2015). *Cranes. General design. Part 1. General principles and requirements*. Helsinki: Suomen Standardisoimisliitto SFS.

SFS-EN-13001-2. (2021). *Crane safety. General design. Part 2. Load actions*. Helsinki: Suomen Standardisoimisliitto SFS.

SFS-EN 13001-3-3. (2014). *Cranes. General design. Part 3-3:Limit states and proof of competence of wheel/rail contact*. Helsinki: Suomen standardisoimisliitto SFS.

SFS-EN 13001-3-2. (2014). *Cranes. General design. Part 3-2: Limit states and proof of competence of wire ropes in reeving systems*. Helsinki: Suomen Standardisoimisliitto SFS.

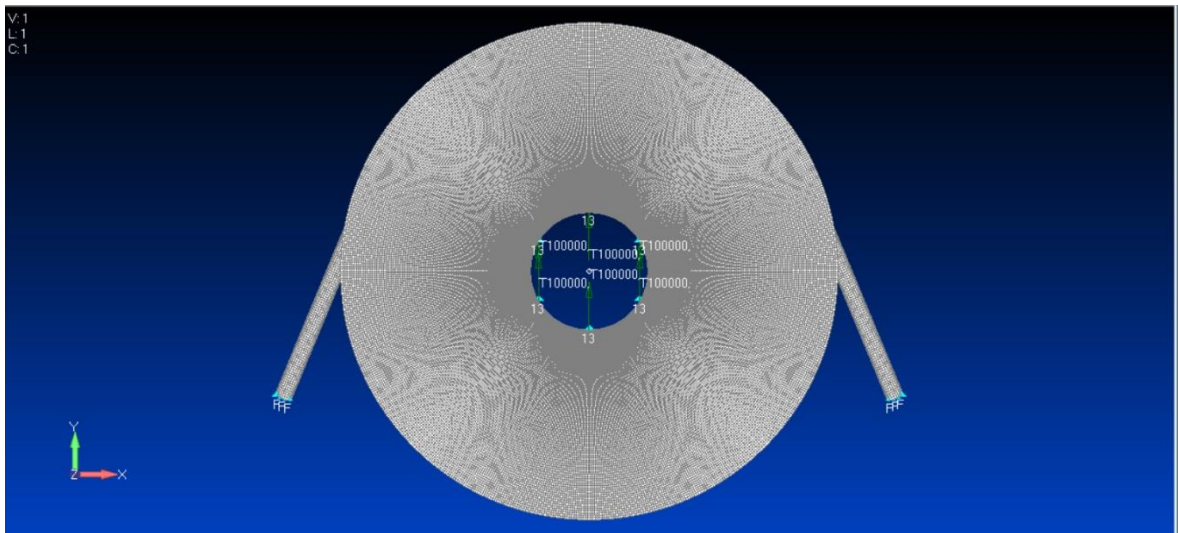
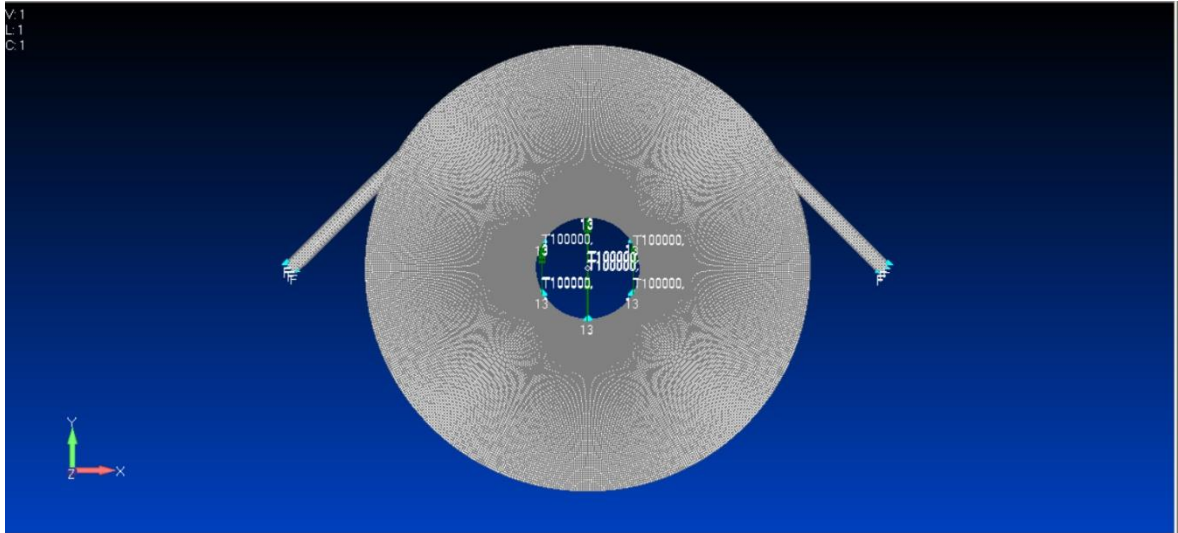
SFS-EN 13001-3-1. (2019). *Cranes. General design. Part 3-2: Limit states and proof of competence of steel structure*. Helsinki: Suomen Standardisoimisliitto SFS.



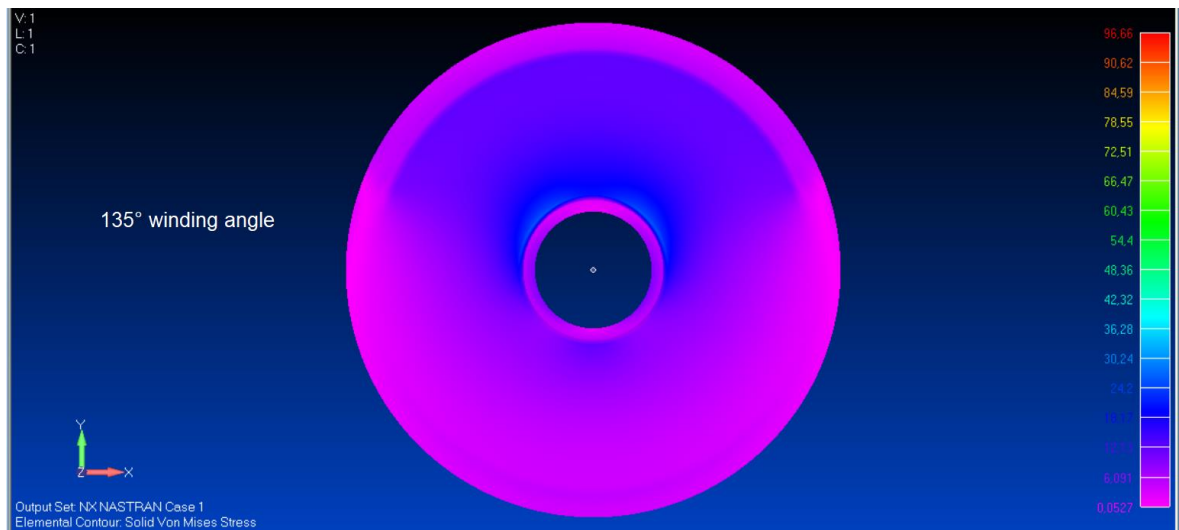
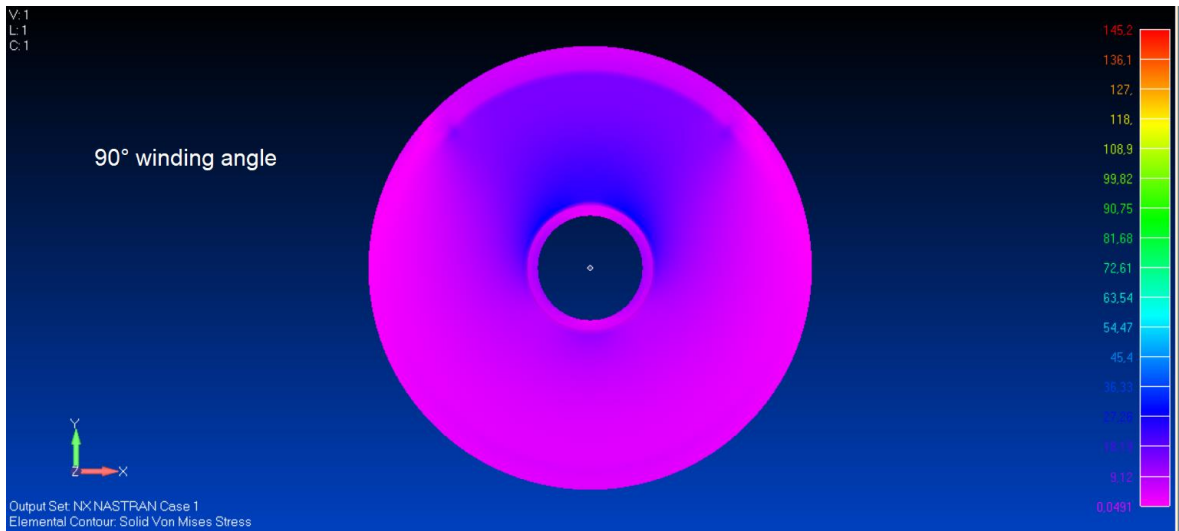
Usabiaga. H., Ezkurra. M., Madoz. M.A., Pagalday. J.M., (2008). Experimental test for measuring the normal and tangential line contact pressure between wire rope and sheaves. *Experimental techniques*. Vol.32 (5), p.34-43

Xi. S., Yalu. .P, Xiaolong.. M, (2016). Modeling and analysis of the rope-sheave interaction at traction interface. *Journal of applied mechanics*. Vol.84

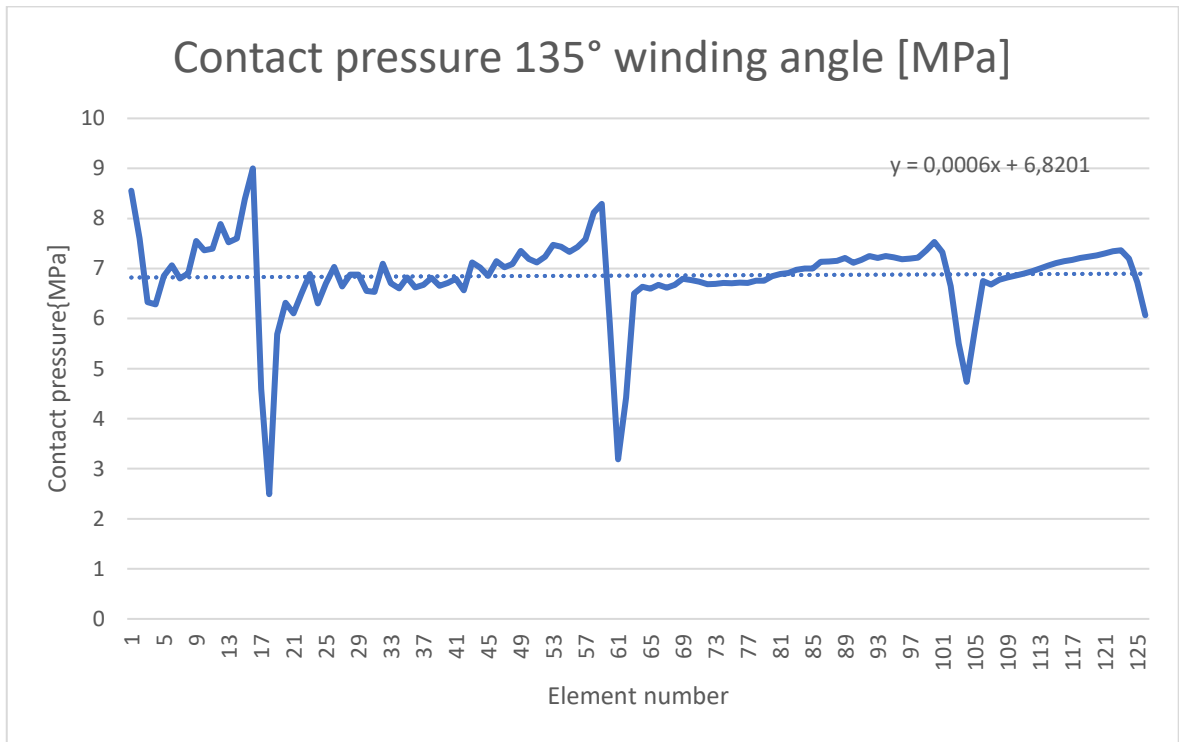
Appendix 1. FE-models of 135° and 90° winding angle sheaves. (FEMAP v11.4.2)



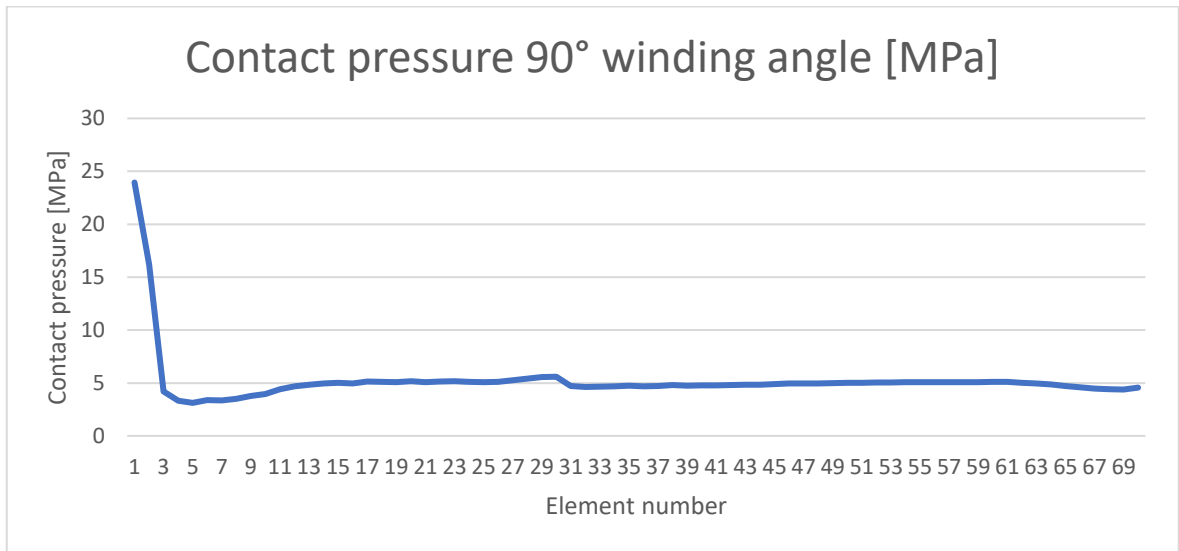
Appendix 2. Von Mises stress distribution in 135° and 90° sheave models. (FEMAP v11.4.2)



Appendix 3. Unfiltered contact pressure curve for 135° winding angle.



Appendix 4. Unfiltered contact pressure curve for 90° winding angle.



Appendix 5. Transverse contact pressure curves.

